JACS
JOURNAL OF THE AMERICAN CHEMICAL SOCIETY
Article
pubs.acs.org/JACS

Structural Study of Citrate Layers on Gold Nanoparticles: Role of Intermolecular Interactions in Stabilizing Nanoparticles

Jong-Won Park and Jennifer S. Shumaker-Parry*

Department of Chemistry, University of Utah, 1400 East 315 South RM 2020, Salt Lake City, Utah 84112, United States

Supporting Information

ABSTRACT: The structure of citrate adlayers on gold nanoparticles (AuNPs) was investigated. Infrared (IR) and X-ray photoelectron spectroscopy (XPS) analyses indicate citrate anions are adsorbed on AuNPs through central carboxylate groups. A unique structure of adsorbed citrate is determined, and a pH-induced structural transition is presented. IR analysis probes dangling dihydrogen anions ($H_2Citrate^-$) and hydrogen bonding of carboxylic acid groups between adsorbed and dangling citrate anions. A contribution of steric repulsion between citrate layers to particle stability is characterized. Structure-based modeling, which is consistent with scanning tunneling microscopy (STM) and transmission electron microscopy (TEM) images in the literature, suggests organization details relating to the formation of self-assembled layers on (111), (110), and (100) surfaces of AuNPs. Adsorption characteristics of the citrate layer include the interaction between hydrogen-bonded citrate chains, bilayer formation, surface coverage, and chirality. The enthalpic gain from intermolecular interactions and the importance of molecular structure/symmetry on the adsorption are discussed. Combining the enthalpic factor with surface diffusion and adsorption geometry of (1,2)-dicarboxyl fragments on Au(111), $H_2Citrate^-$ anions effectively stabilize the (111) surface of the AuNPs. The detailed understanding of intermolecular interactions in the molecular adlayer provides insight for nanoparticle formation and stabilization. We expect these findings will be relevant for other nanoparticles stabilized by hydroxy carboxylate-based amino acids and have broad implications in NP-based interfacial studies and applications.

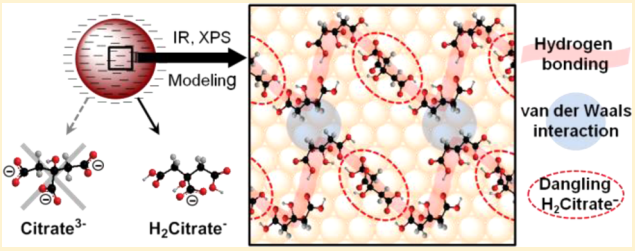

INTRODUCTION

One of the most common synthetic methods for preparation of gold nanoparticles (AuNPs) is based on citrate reduction and stabilization, called the Turkevich method.[1,2] Citrate anions reduce gold ions to atoms and stabilize colloidal AuNPs (i.e., typically 10−100 nm in diameter) formed from clustered atoms. Citrate-stabilized AuNPs (Cit-AuNPs) are commonly employed as tunable foundational materials for a wide range of AuNP-based interfacial studies and applications including nanoparticle assembly,[3,4] particle aggregation,[5] surface charge,[6] linker conjugation,[7] particle growth mechanisms,[8] nanoparticle catalytic activity,[9] ligand exchange reactions,[10] and intracellular activity.[11] Despite a large number of investigations focused on utilizing Cit-AuNPs, the structural details of citrate anions adsorbed on the AuNP surface are still unknown. It is known only that citrate anions coordinate to the metal surface by inner-sphere complexation of the carboxylate groups and there are trace amounts of $AuCl_4^-$, Cl^-, and OH^- on the metal surface.[12,13] A more detailed understanding of the conformation of the adsorbed citrate molecules can aid in addressing questions related to a number of interfacial phenomena observed for Cit-AuNPs.

Moreover, the role of citrate anions in stabilizing the surface of metal NPs (MNPs) is usually approached in an oversimplified manner, likely due to a lack of details regarding the conformation of the citrate molecules adsorbed on MNPs. There are several studies focused on the stability of Cit-AuNPs[12,14] during particle formation,[13,15] but the negatively charged citrate anions have been assumed to act as individual, noninteracting adsorbed species on the surface of MNPs. The formation of a citrate adlayer composed of interacting citrate molecules as a stabilizing layer has never been incorporated in nucleation and growth pathways for nanoparticle formation,[8] and potential intermolecular interactions between citrate anions during nanoparticle growth are typically neglected.[16] In addition, the most important experimental factor in the Turkevich method is still not completely established. The ratio of the gold ion and citrate concentrations used in the reaction has been observed to be a crucial factor for controlling the size of Cit-AuNPs,[2] but it was recently found that changes of other reaction conditions[15,17,18] including solution pH[19] and chloride ion concentrations[20] exclusively govern the size tunability. The structure of the citrate layer on the AuNP surface may be a key factor in gaining a more detailed understanding of nanoparticle formation and stabilization.

Herein, we present a study of the conformation of citrate molecules adsorbed on AuNPs using attenuated total reflectance infrared spectroscopy (ATR-IR) and X-ray photoelectron spectroscopy (XPS). We analyzed spectral responses from

Received: September 30, 2013
Published: January 14, 2014

   dx.doi.org/10.1021/ja4097384 | J. Am. Chem. Soc. 2014, 136, 1907−1921

citrate anions upon pH increase, H/D exchange, additions of alkanethiols and lead ions, and removal of excess layers from AuNPs. Our studies of the coordination of the carboxylate and hydroxyl groups reveal that a specific coordination of adsorbed citrate is dominant.[21] In addition to coordinated citrates, IR analyses also indicate that there are dangling citrate species that are not in direct contact with the metal surface. We discuss intermolecular interactions between the adsorbed and dangling citrate anions. We also present a study of self-assembled layers of citrate molecules on AuNP surfaces combining the spectroscopy results with structure-based modeling in addition to observations described in the literature. Based on the modeling result, we propose formation of citrate chains on AuNP (111), (110), and (100) surfaces and discuss detailed characteristics of the citrate layer. We expect that the detailed description of citrate layers on AuNPs will provide a foundation for additional studies related to the effects of organic adlayers on many different interfacial properties of MNPs, including anisotropic particle growth.[22−24]

RESULTS

Investigation of Stretching Vibrations of Carboxylate Groups of Purified Cit-AuNPs. Our approach to a structural study of citrate layers on AuNP surfaces is based on characterization of coordination of adsorbed citrate species directly in contact with the metal surface, followed by identification of intermolecular interactions between the adsorbed citrates and/or citrate species that were not in contact with the metal surface. We used a combination of IR spectroscopy and XPS to characterize the interactions of citrate molecules on the surfaces of AuNPs. First, we focus on IR analysis to identify the binding nature of the carboxyl groups of citrate molecules on the AuNP surface. The vibrational frequencies of carboxylate groups are highly dependent on coordination modes, such as η^1-COO^-, η^2-COO^- bridging, and η^2-COO^- chelating while the characteristic hydrogen bonds between protonated carboxylic groups are indicative of intermolecular interactions of the adsorbed molecules. Prior to IR analysis, any excess citrate layers on AuNPs were removed by interrupting the intermolecular interactions of COOH hydrogen bonds in a basic condition of pH ∼9 where deprotonated COO^- groups repel each other[25] (see the Supporting Information for effects of hydroxide ions on adsorbed citrate anions, Figures S1−S3). Thus, the resulting IR spectral features should originate from citrate species coordinated directly with the AuNP surface.

Figure 1 presents IR spectra measured using an ATR-IR approach. The film of Cit-AuNPs dispersed on the ZnSe ATR crystal gave rise to intense carboxylate peaks of the adsorbed citrate molecules indicative of asymmetric/symmetric COO^- stretching vibrations (see the Supporting Information for discussion about surface selection rules and intense IR bands of adsorbates on metal nanoparticles in ATR-IR measurements). Typically, the carboxylate group exhibits an asymmetric and a symmetric stretching vibration around 1500−1630 and 1305−1415 cm^{-1}, respectively.[26] The ATR spectra of purified Cit-AuNPs show three distinct peaks, the asymmetric COO^- stretching vibrations ($\nu_{asy}(COO^-)$) at 1611, 1593, and 1558 cm^{-1}, and three other peaks assigned to symmetric COO^- stretching vibrations ($\nu_{sym}(COO^-)$) at 1405, 1394, and 1370 cm^{-1} (Figure 1). Spectra, which were collected at different time periods to probe the changes as water evaporated from the AuNPs dispersed on the ATR crystal, show $\nu(COO^-)$ vibrations, and those vibration bands are relatively sharp and distinguishable (Figure 1A). The vibrational peaks broaden once the film of

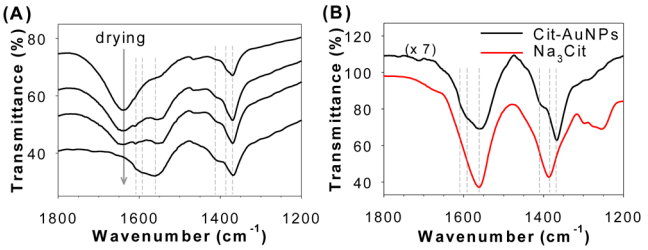

Figure 1. ATR-IR spectra of purified Cit-AuNPs. (A) Each spectrum was collected at a different time period after dispersing the AuNPs on the ATR crystal, showing changes due to water evaporation. Transmittance levels are as recorded. Peaks of the $\nu_{asy}(COO^-)$ at 1611, 1593, 1558 cm^{-1} and $\nu_{sym}(COO^-)$ at 1405, 1394, 1370 cm^{-1} appear (dotted lines). The broad band at 1635 cm^{-1} is a water-bending vibration. (B) Comparison of ATR-IR spectra of the Cit-AuNPs and pure trisodium citrate (Na_3Cit). Note that peak positions are different.

AuNPs is completely dried, but the positions remain constant. While two $\nu_{asy}(COO^-)$ at 1611 and 1558 cm^{-1} and two $\nu_{sym}(COO^-)$ at 1405 and 1370 cm^{-1} are more pronounced, the $\nu(COO^-)$ at 1593 and 1394 cm^{-1} are resolved at the end and beginning of the drying step, respectively. A peak at 1540 cm^{-1} can be due to another type of $\nu_{asy}(COO)^-$, which may result from binding to different facets of the AuNPs. Although these spectral features are similar to those for pure trisodium citrate (Na_3Cit) possessing the $\nu(COO^-)$ at 1575 and 1385 cm^{-1} (Figure 1B; see the Supporting Information for IR bands of purified Cit-AuNPs and Na_3Cit in the entire spectral region and related references) due to ionic coordination with Na^+,[27] the peak positions of the $\nu(COO^-)$ vibrations are different in the two cases. Two additional $\nu_{asy}(COO^-)$ at 1611 and 1558 cm^{-1}, as well as the asymmetric shape of the $\nu_{sym}(COO^-)$ peak with a shoulder centered at ∼1390 cm^{-1}, indicate the presence of at least three types of $\nu(COO^-)$ vibrations for the Cit-AuNPs.[28,29] From the analysis, the IR spectra indicate that the $\nu(COO^-)$ frequencies are split into three distinct peaks for adsorbed citrate molecules on the AuNPs.

Typically, the bending vibrations of adsorbed water ($\delta(OH)_{H2O}$) on metal surfaces are observed in the range of 1610−1650 cm^{-1}, and thus the sharp peak at 1611 cm^{-1} often is assigned to the $\delta(OH)_{H2O}$ free from hydrogen bonding.[30] Instead, the $\delta(OH)_{H2O}$ was observed at ∼1635 cm^{-1}, which is supported by the decrease in amplitude during water evaporation (Figure 1A). In order to probe the spectral contribution from water for the peak at 1611 cm^{-1}, D_2O/NaOD was used to rinse the AuNPs. In this deuterated condition, the $\nu_{asy}(COO^-)$ still appears at 1620 cm^{-1}, which confirms that the peak does not originate from water (Figure S4, Supporting Information). The different interaction of D_2O with COO^- groups may cause the shift in the $\nu_{asy}(COO^-)$ at 1611 cm^{-1} to a higher wavenumber at 1620 cm^{-1}. Typically, upon change of H_2O solvent to D_2O the $\nu_{asy}(COO^-)$ of deprotonated carboxylate groups shifts to a higher frequency by 5−13 cm^{-1}.[31,32]

Identification of Free Carboxylate Groups. In order to distinguish between surface-coordinated and free carboxylate groups on the surface of the AuNPs, Pb^{2+} was added to the solution of purified Cit-AuNPs. The $\nu_{asy}(COO^-)$ of the free carboxylate is expected to shift away from the broadened $\nu_{asy}(COO^-)$ region to about 1515 cm^{-1} (η^2-COO^- chelating[33]) or 1540 cm^{-1} (η^2-COO^- bridging[34]) upon coordination with Pb^{2+}, while the frequency of the coordinated carboxylate should remain at the same position. We observed that the peak at 1593

dx.doi.org/10.1021/ja4097384 | J. Am. Chem. Soc. 2014, 136, 1907−1921

cm^{-1} is significantly attenuated with introduction of Pb^{2+} ions (Figure 2A). In addition, new broad peaks centered at 1540 cm^{-1}

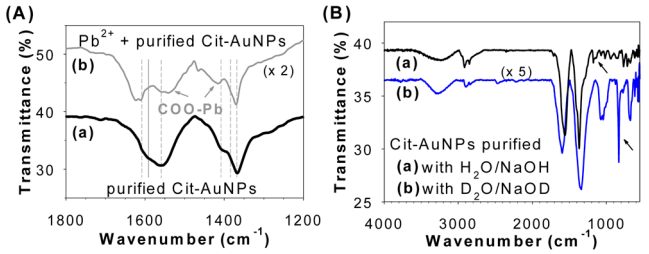

Figure 2. (A) ATR IR spectra of (a) purified Cit-AuNPs and (b) Pb^{2+} treated Cit-AuNPs. Note that the peak around at 1593 cm^{-1} disappears (a solid line in the region of the $\nu_{asy}COO^{-}$), and new peaks at 1540 cm^{-1} and 1417 cm^{-1} appear upon Pb^{2+} addition (arrowed). (B) ATR-IR spectra of Cit-AuNPs purified by (a) H_2O/NaOH and (b) D_2O/NaOD. Note that the $\delta(OH)_{alch}$ at 1175/1145 cm^{-1} is shifted to $\delta(OD)_{alch}$ at 877/833 cm^{-1} upon deuteration (arrow).

and 1417 cm^{-1} appear, which are assigned to the $\nu_{asy}(COO^{-})$ and $\nu_{sym}(COO^{-})$ of the free carboxylate due to η^2-COO^{-} bridging coordination with Pb^{2+} ions.[34] The $\nu_{sym}(COO^{-})$ around 1390 cm^{-1}, where the $\nu_{asy}(COO^{-})$ appears at 1593 cm^{-1}, is difficult to resolve due to other strong $\nu_{sym}(COO^{-})$ bands. In comparison with an $\nu_{asy}(COO^{-})$ of common aliphatic carboxylate groups[35] at ~1550 cm^{-1}, the relatively high $\nu_{asy}(COO^{-})$ of the free carboxylate at 1593 cm^{-1} may originate from an intramolecular hydrogen bonding with the hydroxyl group.[36] The peak at ~1630 cm^{-1} is the $\delta(OH)_{H2O}$ as previously assigned. Thus, the band shift indicates that there is a free carboxylate group in the citrate molecules adsorbed on AuNP surfaces.

Coordination Character of the Binding Carboxylate Groups. AuNPs have facets, and the Au(111) surface typically is the most populated facet in a large AuNP.[37] Since the spectral difference of the distinct $\nu(COO^{-})$ with respect to the crystal facet is known to be less than 15 cm^{-1} as observed for single-crystal electrodes of Pt(*hkl*)[38] and negligible for Au(*hkl*),[39] the observed positions of the $\nu(COO^{-})$ result from the unique binding modes of carboxylate rather than from varied AuNP facets. The IR spectra show two nonequivalent coordinations of carboxylates of adsorbed citrates.[28,29] In Figure 1A, the peaks at 1611 and 1370 cm^{-1} are attributed to a η^1-COO^{-} binding[40,41] on a Au surface,[42] whereas the peaks at 1558 and 1405 cm^{-1} are associated with a η^2-COO^{-} coordination on a Au surface.[39,43−46] These observed vibrational frequencies of the coordinated carboxylate groups also match with computational results for planar gold single crystal surfaces.[42,43] In general, the $\Delta\nu$, $\nu_{asy}(COO^{-}) - \nu_{sym}(COO^{-})$, is indicative of the binding character of a carboxylate group with a metal ion.[47] The $\Delta\nu$ values of the η^1- and η^2-COO^{-} groups of the adsorbed citrate are 241 and 153 cm^{-1}, respectively. These values are in good agreement with the coordination nature of COO^{-} groups with a metal.

Spectra collected after deuterium exchange also were consistent with the nature of the carboxylate coordination on the gold surface relating to interaction with water. Compared with the $\nu(COO^{-})$ vibrations of citrate on AuNPs under the normal conditions, the $\nu(\eta^2$-$COO^{-})$ at ~1558/1405 cm^{-1} did not shift, and the $\nu_{asy}(COO^{-})$ of the free carboxylate group appeared at the same frequency of ~1593 cm^{-1}, due to a lack of interactions with water molecules. The former is associated with the coordination of both oxygen atoms to metal surfaces, and the latter is related to the intramolecular interaction with the hydroxyl group of the adsorbed citrate. However, when one oxygen atom of the η^1-COO^{-} group interacts with water molecules, hydrogen bonding of the oxygen atom with D_2O[48] may shift the $\nu_{sym}(COO^{-})$ to higher frequency[31,32] at 1620 cm^{-1} (Figure S4, Supporting Information). The broadened peaks of the asy/sym $\nu(COO^{-})$ vibration by use of D_2O also are consistent with various hydrogen-bond configurations.[48]

Coordination of the Alcoholic OH Group. In addition to the carboxylates, we studied the coordination of the alcoholic group of adsorbed citrate. In most studies of citrate conformation on a metal surface, the binding of the citrate hydroxyl group has been neglected. The hydroxyl group of citrate is well-known for 5-membered chelating coordination to metal atoms.[40,49] With this in mind, the coordination of the hydroxyl group of citrate to the surface of AuNPs should be considered. While methanol and/or ethanol molecules coordinate to small noble metal clusters ($n \leq 15$) without O−H bond cleavage,[50] the hydroxyl groups of methanol[51] and ethanol[52] have been reported to be cleaved during alkoxide formation on a metal surface, and it was suggested that ethoxide adsorbed on a Au surface is not stable at room temperature.[52]

We observed $\nu(C-O)_{alch}$[26,53] of the alcohol (alch) group at 1137, 1111, and 1076 cm^{-1} for pure trisodium citrate and the shift of those peaks to 1070 cm^{-1} for the Cit-AuNPs (see the Supporting Information, Figures S1 and S5). The shift of $\nu(C-O)_{alch}$ has been used as evidence for alcohol coordination to gold clusters.[50] Depending on the size and charge of the gold cluster as well as the type of alcohol (e.g., methanol or ethanol), the $\nu(C-O)_{alch}$ of a gold−alcohol complex decreases by 25−60 cm^{-1} compared to a free alcohol in the gas phase. For larger nanoparticles or a planar surface of metal oxides, the $\nu(C-O)_{alch}$ shift also has been employed as a probe to determine the alcohol group coordination.[54] In our study, we observed a new $\nu(C-O)_{alch}$ at 1070 cm^{-1}, but we did not conclude the shift of the $\nu(C-O)_{alch}$ was due to the coordination of the OH group to the Au surface since $\gamma(CH_2)$ and $\nu(C-C)$ are probably shifted around the $\nu(C-O)_{alch}$ region simultaneously upon citrate adsorption on the AuNP surface due to the resultant conformational change.[55] Therefore, more experimental evidence is required for determination of the involvement of the citrate hydroxyl group in coordination on the AuNP surface.

In order to further probe the coordination of the citrate hydroxyl group, we investigated the IR spectrum of purified Cit-AuNPs using a deuterium exchange experiment (Figure 2B). NaOD and D_2O in the purification step of the Cit-AuNP were used instead of NaOH and H_2O, and the pH was adjusted to ~9 where protonated carboxylic species are present at a minute level and a spectral change is expected from hydroxyl groups. The most distinct features of the spectrum are the appearance of a strong $\delta(OD)_{alch}$[56] peak at 877/833 cm^{-1} as well as the disappearance of the counterpart peak of the $\delta(OH)_{alch}$ located at 1175/1145 cm^{-1}.[57,58] The 1175/1145 cm^{-1} peaks are not attributed to a $\delta(OH)$ vibration from −COOH groups because most of the carboxylic acid groups are deprotonated at pH 9. Also, the intensities of the peak at 833 cm^{-1} for the deuterated Cit-AuNPs and the peak at 1175 cm^{-1} for the Cit-AuNPs do not change significantly as samples are dried (see the Supporting Information, Figures S5 and S6). Consistent vibrational features indicate those vibrational bands stem from an identical vibration mode. This observation verifies the existence of a free hydroxyl

dx.doi.org/10.1021/ja4097384 | J. Am. Chem. Soc. 2014, 136, 1907−1921

group of the adsorbed citrate that does not participate in metal complexation and is available for other interactions.

XPS Characterization of Adsorbed Citrate. We employed XPS for further analysis of the surface chemistry of Cit-AuNPs. The binding energy (BE) of electrons of an atom is sensitive to the local electronic state of adjacent atoms and provides information about binding and coordination of functional groups. We used XPS to analyze a drop-cast film of the purified Cit-AuNPs and Na_3Cit on silicon wafer substrates in order to probe the coordination of carboxylic acid and hydroxyl groups. The binding energy of the C 1s for adventitious carbon as a reference is 284.8 eV. The deconvoluted C 1s spectrum consists of four distinct binding energies at 284.8, 285.9, 287.6, and 289.4 eV, which are attributed to adventitious carbons (C−C or C−H), the hydroxyl ($C-OH_{alch}$)[59] and/or the α-carbons (CH_2),[60] the coordinated carboxylates (COO−Au),[61] and free carboxyl moieties (COOH[62] or COO^-),[60] respectively (Table 1; see also the Supporting Information, Figure S7). Two carboxylate peaks can be identified depending on coordination to a Au surface, which is consistent with IR analysis in this study (see Supporting Information, Figure S8 and ionic nature of COO−Au interaction). A dominant peak of carboxylic acid groups at 288.2 eV for the pure Na_3Cit also is located in the coordinated COO^- regime, and this peak is due to Na^+-coordinated carboxylate groups.[27] Observation of the uncoordinated carboxylate of adsorbed citrate anions indicates that most of the free carboxylate groups do not interact with Na^+ ions on the surface. The previous IR analysis based on the $\delta(OH)_{alch}$ shift upon deuteration demonstrated only the presence of uncoordinated alcohol groups of adsorbed citrate species without O−H cleavage. Because a coordinated alcohol group after O−H cleavage is expected to be undetectable under the deuterated IR analysis, the regions of the XPS C 1s were analyzed to determine the presence of binding alcohol species. Although the C 1s binding energy of the C−OH regime in this measurement is located within the C−OH coordinate, a conclusion cannot be made about the C−OH binding on the Au surface because the CH_2 binding energy overlaps the region of the single peak observed in the XPS spectrum. The peak cannot be deconvoluted into two components due to the intrinsic low concentration of the adsorbed citrate.[63] As a result, the presence of adsorbed citrate with the hydroxyl group coordinated to the surface cannot be excluded by XPS analysis or the IR study, but we probed the coordination of the hydroxyl group at a pH above 11 (see the following result and the Discussion; see also Figure 5B and related discussion).

Table 1. C 1s Binding Energy of Purified Cit-AuNPs and Pure Trisodium Citrate

C 1s BE (eV)	COH/CH_2	COO-Au	COO^-Na^+	free COO(H)
Na_3Cit	286.3		288.2	289.3
Cit-AuNPs	285.9 (0.1)	287.6 (0.3)		289.4 (0.2)

The number in parentheses is the standard deviation.

Spectral Change of the Vibrational Bands for Adsorbed Citrate under Basic Conditions. We observed a significant change of IR peaks from thiol-functionalized Cit-AuNPs in basic solution conditions. First, the surface of Cit-AuNPs was functionalized with ω-terminated alkyl or aryl thiols. The pH of the solution of AuNPs was adjusted to above 11 through addition of NaOH. New IR peaks at 2985, 2976, 1614, 1371, 1349, 1310, 1108, 1077, 825, and 583 cm^{-1} appear when the pH is higher than 11 for functionalized AuNPs with HOOC-Ph-SH or CH_3-C_{11}-SH thiols (Figure 3). Magnified spectra are presented in Supporting Information (Figure S9). Those peaks disappear after the samples are completely dried. As discussed below, those peaks are not related to the thiols and should be associated with citrate molecules (see the Supporting Information for exclusion of the possibility of ethanol derivatives and carbonate ions, Figure S10).

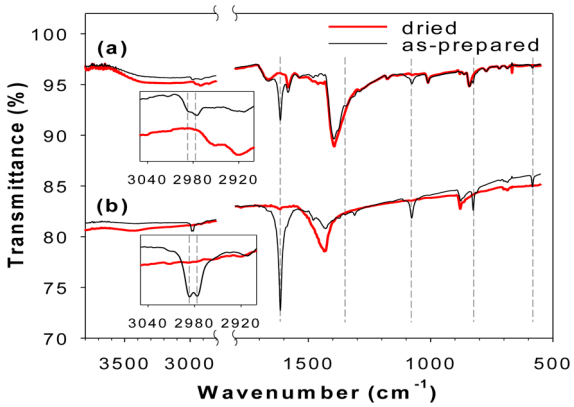

Figure 3. Transmission IR spectra of functionalized Cit-AuNPs by (a) HOOC-Ph-SH and (b) CH_3-C_{11}-SH thiols when the pH > ~11. Bands marked with dashed lines are unique to this pH (black spectra), and those bands disappear after samples are dried (red spectra). The bands are located at 2985 (inset), 2976 (inset), 1614, 1371 (not indicated), 1349, 1310 (not indicated), 1108 (not indicated), 1077, 825, and 583 cm^{-1}. Traces (a) are offset from a baseline by 13%.

Under these basic pH conditions, the IR data are consistent with citrate configurations for the binding of the free terminal carboxylate group to the AuNP surface. The asy/sym $\nu(COO^-)$ vibrations at 1611/1370 cm^{-1} indicate a η^1-COO^- binding to the surface. The CH_2 stretching is located at 2985/2976 cm^{-1}.[26] The peaks at 1108 and 1077 cm^{-1} can be assigned to a $(C-O)_{alch}$ stretching,[26,53] a C−C stretching[64] and/or a CH_2 wagging vibration,[65] which are newly exhibited after a structural change of adsorbed citrate on the Au surface. The relatively strong in-plane COO^- rocking[66] at 583 cm^{-1} can be correlated to a terminal COO^- coordination combined with an in-plane COO^- scissoring[66] at 825 cm^{-1}. Overall, the IR data indicate a structural transformation of adsorbed citrate relating to coordination of all carboxylate groups. This may be accompanied by coordination of the hydroxyl group.

IR Frequencies Indicative of Hydrogen Bonds in the Citrate Layer on AuNPs. Until now, coordination of adsorbed citrate species directly in contact with the metal surface was investigated. For the experiments described above, purification of Cit-AuNPs was performed under basic conditions (pH ~9) in order to disrupt any intermolecular hydrogen bonds between citrate layers through deprotonation of the carboxylic acid groups. Under such conditions, only citrate species adsorbed directly on the AuNP surface should remain. Here, we investigated intermolecular interactions between the adsorbed citrates and/or potential citrate species that are not in contact with the metal surface. A characteristic peak of the hydrogen bond between carboxylic acid groups centered at 1710 cm^{-1} was observed for Cit-AuNPs that were not purified under basic conditions (see the Supporting Information, Figure S11A). This indicates the presence of intermolecular interactions between surface citrates and possibly with other oxidized species of citrate.

dx.doi.org/10.1021/ja4097384 | J. Am. Chem. Soc. 2014, 136, 1907−1921

We investigated the hydrogen bonds of a layer of citrate anions on AuNPs in more detail. As a first step, excess citrate anions and other molecules remaining in the Cit-AuNP solution were removed. Use of ethanol or acidic water to attempt to purify the Cit-AuNPs resulted in irreversible aggregation of the AuNPs during repeated centrifugations and particle dispersion steps. In order to stabilize the Cit-AuNPs while retaining any potential multilayer structure of citrate during the rinsing step with EtOH, the adsorption of the alkanethiols at submonolayer coverages on the Cit-AuNPs was used. Cit-AuNPs were functionalized with 1/4−1/2 stoichiometric amounts of alkanethiols relative to monolayer coverage so that adsorbed citrate would be preserved on the remaining 1/2−3/4 of the surface area on AuNPs. We assumed that all of the added alkanethiols are adsorbed on the surface prior to a complete monolayer formation due to the large adsorption constant (K_{eq} = ~10^7).[67] Relatively long alkanethiols (CH_3−C_{11}-SH) were used to impart stability under the solution conditions and should not interact with the carboxylic acid groups of citrate or form intermolecular hydrogen bonds in regions where the citrate layer is not displaced. By this purification method, we removed physisorbed citrate and other molecules remaining from the AuNPs synthesis and investigated the structure of the remaining citrate layer on the AuNPs. Characteristic ν(C═O) peaks of COOH hydrogen bonds at 1734 and 1704 cm^{-1} were observed in the partially alkanethiol-functionalized AuNPs, which are assigned to the formation of acyclic and cyclic COOH dimers,[34] respectively (see the Supporting Information, Figure S12). Notably, the ν(C═O) of noninteracting COOH at 1764 cm^{-1} was not detected (Figure S1).

In addition, it is possible that an interaction of carboxylic acid groups with water molecules exists. Another report indicated that a water molecule is expected to interact with two free carboxylic acid groups of adsorbed citrate anions on AgNPs.[16] This type of intermolecular interaction (−COOH···H_2O···HOOC−) should exhibit sharp hydrogen-bonding peaks of $\nu(O-H)_{H2O}$ around 3548−3414 cm^{-1} and $\nu(O-H)_{COOH}$ around 3230 cm^{-1}, respectively.[68] However, the IR spectrum of Cit-AuNPs shows only broad peaks around those frequencies, which indicates that an inclusion of water molecules between two carboxylic acid groups of adsorbed citrate is not a dominant formation. Therefore, we concluded that water molecules do not play a critical role in hydrogen bonding with carboxylic acid groups of citrate molecules adsorbed on AuNPs.

IR Analysis for Dangling Citrate Anions as Another Molecular Layer on AuNPs. Thiol functionalization of Cit-AuNPs led to the characterization of COOH/COO^- interactions between citrate anions without significantly disrupting the intermolecular hydrogen bonds in the citrate layer. The IR data indicate that there are both thiol layers and hydrogen-bonded citrate layers on AuNPs. Addition of thiols to Cit-AuNP solutions leads to coadsorption of thiols between citrate layers rather than complete displacement of adsorbed citrate, and this also enabled us to investigate the structure of citrate layers. A detailed mechanism of thiol coadsorption on Cit-AuNPs will be discussed in a future article.[69]

Figure 4A presents spectra to compare $\nu_{asy}(COO^-)$ vibrations before and after addition of alkanethiols to the solution of Cit-AuNPs as prepared. The thiols used in the functionalization are in excess (~530 times) compared to a monolayer coverage on the AuNPs. The $\nu_{asy}(COO^-)$ at ~1590 cm^{-1} is pronounced for as-prepared Cit-AuNPs. Notably, the peak at ~1590 cm^{-1} disappeared and the peak at 1611 cm^{-1} became more intense

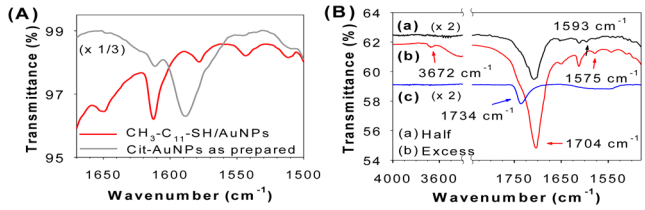

Figure 4. ATR-IR spectra of partially functionalized Cit-AuNPs by methyl-terminated alkanethiol (CH_3−C_{11}-SH). (A) Comparison of as-prepared Cit-AuNPs before and after functionalization with an excess of CH_3−C_{11}-SH thiol at the frequency region of $\nu_{asy}(COO^-)$ vibrations. (B) The amount of thiol added to the AuNP solution is adjusted to functionalize (a) half of the total surface area on the AuNPs and (b) present in excess (~530 times) compared to a monolayer coverage. The red-arrowed peaks at 3672, 1704, and 1575 cm^{-1} originate from organized citrate overlayers. Spectrum (c) was collected after addition of the excess of CH_3−C_{11}-SH into purified Cit-AuNPs, which shows ν(C═O) only at 1734 cm^{-1} (blue arrow).

after the thiol addition. This indicates removal of physisorbed citrate and its oxidized species possessing COO^- groups and a possible η^1-COO^- binding of the terminal carboxyl group to the surface. The previous peak assignment for the peak at 1593 cm^{-1} to $\nu_{asy}(COO^-)$ of the terminal carboxylate group of adsorbed citrate is consistent with the intensity attenuation of that peak as the amounts of thiols for the functionalization of Cit-AuNPs increase. The characteristic $\nu_{asy}(COO^-)$ peaks indicative of the COO-coordination still appear at 1611 and 1558−1545 cm^{-1} regardless of the addition of the thiol. The $\nu_{sym}(COO^-)$ bands between 1410 and 1370 cm^{-1} are buried by strong CH_2 vibrations as well as C−O−H bending vibrations. The peaks at 1650[70] and 1510[71] cm^{-1} are probably related to various hydrogen bond configurations such as $COO^-\cdots H^+\cdots{}^-OOC$ and $COO^-Na^+\cdots Na^+{}^-OOC$ interactions since those peaks were not observed in the deprotonated condition for carboxyl groups at pH ~9.

The AuNPs functionalized with 1/2 surface-stoichiometric amounts of thiols exhibit a weak peak of the free $\nu_{asy}(COO^-)$ at 1593 cm^{-1} (Figure 4B, see also Figure S13A in the Supporting Information for other frequency regions) and a major peak of the −COOH hydrogen bond at 1704 cm^{-1}. A shoulder band at 1734 cm^{-1} also is visible. When excess thiols were added to the AuNP solution, however, the peak of the COOH hydrogen bond at 1704 cm^{-1} became stronger, and the intensity of a peak at 1575 cm^{-1}, assigned to $\nu_{asy}(COO^-)$, was much pronounced (spectrum b in Figure 4B). In addition, the free terminal carboxylate group at 1593 cm^{-1} disappeared after addition of excess thiols. Interestingly, a non-hydrogen-bonded $\nu(O-H)_{alch}$[72] at 3672 cm^{-1} has been detected (arrowed, spectrum b in Figure 4B). This correlation between the terminal carboxyl and hydroxyl groups implies possible interaction through $OH_{alch}\cdots{}^-OOC$ hydrogen bonds between carboxylate impurities and the citrate layer, which also indicates intermolecular interactions through −COOH··· HOOC− hydrogen bonds between citrate anions. Thiol-functionalization was performed in ethanol solutions, and thus, any EtOH molecules remaining in the AuNP sample are expected to exhibit a $\nu(O-H)_{alch}$ band at the same frequency. However, we can rule out this possibility based on two main reasons. First, any remaining EtOH molecules should interact with each other through hydrogen bonding and therefore a $\nu(O-H)_{alch}$ band from individual EtOH molecules would not be observed.[73] Second, the remaining EtOH molecules would be observed regardless of the type of thiol, but other thiol-

dx.doi.org/10.1021/ja4097384 | J. Am. Chem. Soc. 2014, 136, 1907−1921

functionalized AuNPs did not exhibit the $\nu(O-H)_{alch}$ band. This may be due to interactions of thiol functional groups with the hydroxyl groups of citrate and possible disruption of the citrate layer. Only alkanethiol-functionalized AuNPs exhibit the $\nu(O-H)_{alch}$ band. The adsorption of alkanethiols on the surface may promote the liberation of non-hydrogen-bonded hydroxyl groups of surface citrates through removing weakly adsorbed hydroxyl carboxylate derivatives from the surface. In terms of the enhanced intensity of the peak at 1704 cm^{-1}, the alkanethiol layer may disrupt citrate layers partially, making the orientation of cyclic COOH hydrogen-bonding more IR active with respect to the AuNP surface.[39] The absence of a non-hydrogen-bonded $\nu(O-H)_{COOH}$ of free carboxylic acid groups typically at ~3520 cm^{-1}[74] is consistent with the absence of the $\nu(C=O)$ of noninteracting COOH at 1764 cm^{-1}.

Interestingly, when Cit-AuNPs purified by OH^- ions were functionalized with the alkanethiols, only the $\nu(C=O)$ of acyclic COOH dimers at 1734 cm^{-1} was observed (spectrum c in Figure 4B; see also Figure S13B in the Supporting Information for other frequency regions). Some thiol protons of alkanethiols are eventually transferred to uncoordinated COO^- groups to form COOH dimers. There is no additional layer on the purified Cit-AuNPs, and thus, this suggests adsorbed citrate anions interact only through acyclic −COOH dimerization on AuNP surfaces. The possibility of ionic hydrogen bonding through COOH···$^-$OOC was excluded due to a lack of a broad asymmetric band of $\nu(O-H)_{COOH}$ at a low frequency.[75] The molecule-surface interaction may prevent adsorbed citrate anions from forming cyclic COOH hydrogen bonding.

The correlation between the 3672 cm^{-1} band of free $\nu(O-H)_{alch}$, the 1575 cm^{-1} band of $\nu_{asy}(COO^-)$, and the 1704 cm^{-1} band of $\nu(C=O)_{COOH}$ in Figure 4 indicates the presence of another type of citrate anion different from the adsorbed citrate species and intermolecular hydrogen bonds between both citrate species. This is likely associated with dangling dihydrogen citrate ($H_2Citrate^-$) that is deprotonated on the central carboxylic acid group.[26] The first deprotonation of citric acid ($H_3Citrate$) occurs at the central carboxylic acid.[76] The incorporation of the dangling citrate species into interactions with adsorbed citrate on the surface leads to the appearances of the liberated non-hydrogen-bonded $\nu(O-H)_{alch}$ at 3672 cm^{-1} and the noninteracting central $\nu_{asy}(COO^-)$ of the dangling citrate species at 1575 cm^{-1}. The terminal carboxyl group of adsorbed citrate, exhibiting the intramolecular hydrogen bond with the hydroxyl group upon deprotonation, is hydrogen-bonded with the terminal carboxylic group of the dangling citrate in the citrate adlayer on the as-prepared Cit-AuNPs (see the citrate configurations shown in Figures 5 and 6 in the Discussion and Figure S14 in the Supporting Information). This results in the formation of the hydrogen-bonded cyclic COOH dimers at 1704 cm^{-1}, as well as the liberation of the hydroxyl group into non-hydrogen-bonded $\nu(O-H)_{alch}$ at 3672 cm^{-1}. Adjacent adsorbed citrate anions are also hydrogen-bonded through the formation of acyclic COOH dimers. Thus, the intermolecular interactions in the citrate layer are mediated through the hydrogen bonds of carboxylic acid groups between dangling and adsorbed citrate anions on AuNPs.

DISCUSSION

Conformation of Citrate Anions Adsorbed on AuNPs.

The FTIR and XPS analyses indicate the presence of two distinct binding modes of COO^- groups with one COO^- group freely exposed to solution. Considering this analysis and related results presented in the literature, we expect that the citrate anions adsorbed on a AuNP surface adopt the η^2-COO^- bridging coordination of the central COO^- group and the η^1-COO^- coordination of the terminal COO^- group (Figure 5A,

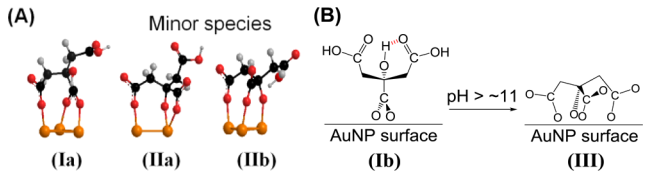

Figure 5. (A) Proposed conformation of adsorbed citrate on purified Cit-AuNPs. Conformation (**I**) is consistent with the IR and XPS analysis, but a mixture of conformations (**I**) and (**II**) also is possible. Uncoordinated carboxyl groups are presented as protonated forms. Orange: gold (representative of the gold surface), red: oxygen, black: carbon, gray: hydrogen. (B) Binding of the hydroxyl and free carboxylate groups of adsorbed citrate on the Au surface when the pH is higher than 11.

conformation Ia). Although it is not possible to distinguish between bridging and chelating coordinations of COO^- groups from IR data,[39] DFT calculations[43] and STM-image analyses[77] indicate that chelating η^2-COO^- coordination is not stable on gold surfaces, transforming to a η^1-coordination. Although there might be an orientation change of the adsorbed citrate due to deprotonation[46] of free carboxylic acid groups as well as changes of the adsorbate concentration[78] and ionic strength,[79] the binding geometry of adsorbed citrate is not expected to be altered significantly after the purification step under basic conditions. The central COO^- coordination plays a key role in the conformation of adsorbed citrate anions. The binding of the central and one terminal COO^- groups of citrate in this configuration is consistent with the proposed citrate conformation on AgNPs[16,28] as well as the suggested preferential binding of citrate to Ag(111) of silver nanoplates.[80] In fact, we estimated ~1/3 of the coordinated terminal COO^- groups actually remain uncoordinated, determined by XPS analysis based on the area ratio of C1s COO(H)/COO-Au for purified Cit-AuNPs (0.8) (Figure S7A, Supporting Information). Therefore, conformation Ib is also possible as another structure of adsorbed citrate anion, and the estimated ratio between conformation Ia and Ib is about 1/2 (Ib/Ia). It is not clear whether this ratio is a consequence of a facet-dependent adsorption structure of citrate anion or a binding equilibrium of the terminal carboxyl groups to the surface.

Due to the intrinsic ensemble nature of IR measurements, a mixture of the possible citrate conformations may produce the vibration characteristics of three different carboxylate groups. When the protonation trend of citrate is considered, the most probable conformations can be identified. Martin has reported that the dihydrogen citrate species ($H_2Citrate^-$) with the central carboxylic acid group deprotonated is the most populated species at the beginning of the deprotonation process of citric acid ($H_3Citrate$).[76] The central carboxylic acid group has the lowest pK_a,[81] and it probably binds on the Au surface preferentially at the beginning stage of citrate adsorption.[82] Although $H_3Citrate$ and $H_2Citrate^-$ are expected to be dominant at the pH ~3.2 condition[83] of the as-prepared Cit-AuNP solution, the protonated carboxylic groups of citric acid can be adsorbed on a Au(111) surface by an anodic reaction associated with oxidation of the Au surface[84] (see the Au oxidation states in XPS data in the Supporting Information, Figure S8), and/or the purification procedure under basic conditions may promote the

dx.doi.org/10.1021/ja4097384 | J. Am. Chem. Soc. 2014, 136, 1907−1921

binding of terminal COOH groups. Regardless of the effect of deprotonation on citrate adsorption, the molecular geometry upon adsorption is likely a critical factor. A lattice match between the spacing of the surface gold atoms and the molecular length of adsorbed moieties of citrate anions may prevent citrate adsorption through both terminal COO^- groups on the Au(111) surface. Yin and co-workers[80] suggested that dicarboxylic acids having more than two methylene ($-CH_2-$) units do not selectively bind to the Ag(111) surface (the surface lattice spacing for silver and gold is 2.89 Å and 2.88 Å, respectively) due to the size mismatch. In this study, the central and a terminal COO^- groups are spaced apart by two carbon atoms (distance between two carbons of the COO^- groups: 3.3 Å), and this length of the molecular moiety for adsorption is commensurate with the lattice spacing of 2.88 Å for Au(111).

We also propose conformation II (IIa: chelating, IIb: bridging) as a minor species (Figure 5A) since we cannot rule out the possibility of the presence of a mixture of conformations I and II based on the IR and XPS results. Both conformations IIa and IIb are associated with coordination of the hydroxyl group. The detection of $\delta(OH)_{alch}$ does not necessarily mean that all of the hydroxyl groups are uncoordinated, and the C 1s binding energy of the hydroxyl group is not sensitive to coordination type due to the low citrate concentration. Conformation IIa is common for citrate-metal complexes, and the crystal structures of various citrate-metal complexes revealed that the hydroxyl group acts as a supporting donor group for the central COO^- coordination. However, conformation II itself does not explain the IR data because an intact hydroxyl group has been detected (see surface binding of the hydroxyl and carboxylate groups for a possible exclusion of conformation II).

Nichols et al. proposed a citrate structure with all three COO^- groups coordinated on a Au(111) surface as a η^2-COO^- mode.[44] They claimed that there was only one symmetric COO^- stretching vibration of a η^2-COO^- coordination at 1385 cm^{-1}, which led to the proposed citrate conformation. Contrary to the aforementioned observation the IR spectra also contain small but noticeable peaks at 1610 and 1555 cm^{-1} as well as a broad peak of $\nu_{sym}(COO^-)$ with a shoulder, which is indicative of a different COO^- coordination. However, an alternative coordination was not discussed. Other reports discuss tridentate citrate binding (η^2-COO^- coordination) to gold surfaces, but questions remain. One example is an interpretation of the STM image of citrate organization on Au(111) by Bai and co-workers[85] that relies on an overestimation of the size of the citrate anion. The estimated lateral length of the proposed citrate conformation based on the STM scale bar is about 10 Å, but the actual size of the tridentate citrate anion is about 5 Å. In another study, Teobaldi and Zerbetto conclude that adsorption of citrate molecules on a Au(111) surface through three η^2-COO^- coordinations may not occur, studied by computer simulation using the tridentate citrate conformation on a planar gold (111).[86] These contradictory results imply that the previously proposed tridentate coordination of citrate is not consistent with experimental results.

Surface Binding of the Hydroxyl and Carboxylate Groups of Adsorbed Citrate. The binding of COO^- groups of adsorbed molecules to gold surfaces has been demonstrated by a change of pH[46] and application of an electric field.[87] The proposed citrate conformation on a AuNP surface via the terminal and the central COO^- groups is further supported by the binding of the free COO^- and the hydroxyl group to the AuNP surface into formation of a tetradentate citrate configuration. The binding of the terminal COO^- group of citrate adsorbed on the AuNP surface was induced through an increase of pH (Figure 5B). This structure (conformation III) was proposed based on IR analysis in the Results (Figure 3). Briefly, the solution pH of alkanethiol-functionalized Cit-AuNPs was increased to above 11. This leads to a significant change of IR bands from citrate molecules. The spectral change indicates that adsorbed citrate anions were transformed into another conformation, and this structural change can be attributed to the binding of the free COO^- group to the AuNP surface. The thiol layer at each particle surface prevents an interparticle-type interaction through the free COO^- groups of adsorbed citrate. The basic pH condition can lead to deprotonation of the hydroxyl group[88] and a common five-membered ring formation to the metal with the hydroxyl and the central COO^- groups. Conformation III is a structural transformation from conformation Ia or Ib via hydroxyl/carboxylate coordinations. We found that the terminal COO^- groups in conformation II are in close proximity to the surface compared to conformation I, and it is reasonable to assume that the deprotonation of the hydroxyl group also induces the binding of both of the terminal carboxylate groups to the surface. Therefore, conformation II may be excluded and considered as an unstable, intermediate form during the structure transition from conformation I to III.

Intermolecular Interactions between Adsorbed and Dangling Citrate Layers on AuNPs. It is known that on a planar Au surface ω-carboxyl alkanethiol forms a double layer by formation of carboxylic acid dimers.[25,89] It is likely that the protonated citrate molecules exhibit similar layer formation on AuNPs. Floate et al. have observed the increased intensity of the COOH peak of citric acid at 1720 cm^{-1} on a Au(111) surface as the deprotonated citrates are adsorbed on the surface, but they found that the COOH peak does not originate from an adsorbed citrate species.[43] This may suggest intermolecular interactions between the adsorbed citrate and another type of citrate anion by COOH hydrogen bonds. Lee et al. observed a two to three molecular layer of citrate on AuNPs by atomic-resolution TEM analysis.[90] Hydrogen bonding of the free COOH groups of citrate molecules plays an important role in formation of citrate layers on the surface of AuNPs.[91]

The IR analysis also indicates the presence of dangling citrate anions and hydrogen bonding between free COOH groups (see Figure 4) which may lead to formation of multiple citrate layers at the surface of the AuNPs. The potential multilayer formation of citrate molecules can be described as intermolecular interactions of the dangling citrate anion with adsorbed citrate species. Figure 6A presents the representation of a citrate trimer, consisting of two adsorbed species and one dangling dihydrogen species. The formation of the citrate trimer is associated with the ordered orientation of hydroxyl groups from the adsorbed and dangling citrate layers, which can generate the distinct peaks of the free $\nu(O-H)_{alch}$ at 3672 cm^{-1}. The citrate configuration in Figure 6A likely represents an ideal configuration of building blocks of surface citrate on AuNPs. Due to a lack of molecule−metal interaction, dangling anions form cyclic COOH dimers with adsorbed anions for the maximum intermolecular interaction but adsorbed anions form only acyclic COOH dimers with adjacent adsorbed anions. Figure 6B illustrates a disordered configuration, resulting from breakage of the intermolecular interactions between the terminal COOH groups by physisorbed alkanethiol layers. The disordered configuration shows noninteracting terminal COOH groups from both the adsorbed and dangling citrate layers, which are accompanied with less pronounced

dx.doi.org/10.1021/ja4097384 | J. Am. Chem. Soc. 2014, 136, 1907−1921

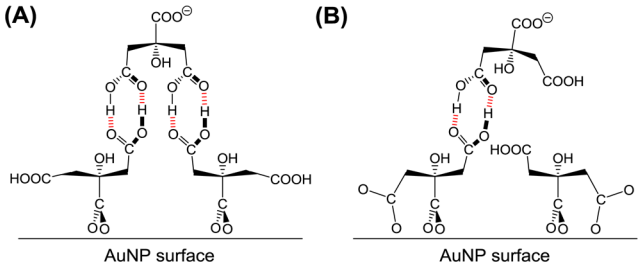

Figure 6. Proposed configuration of a unit of citrate trimer consisting of two adsorbed and one dangling species as building blocks of surface citrate adlayers on AuNPs. (A) Ideal organization leads to formation of a citrate bilayer; adsorbed anions are hydrogen-bonded with adjacent adsorbed anions through formation of acyclic COOH dimers. (B) A disordered citrate trimer is associated with noninteracting terminal COOH and η^1-COO^- groups.

hydrogen bonds between −COOH groups and possible interactions of the hydroxyl groups with the terminal COOH groups. The IR spectrum of as-prepared Cit-AuNPs exhibits the characteristic ν(C−H) vibrations of H_3C- and $-CH_2-$ moieties (Figure S11A, Supporting Informatin), and thus acetoacetic acid (CH_3COCH_2COOH), rather than acetone dicarboxylic acid ($HOOCCH_2COCH_2COOH$), is likely a major oxidized species of citrate adsorbed on AuNPs. The C 1s area ratio of COOH/(COO-Au + COO^-Na^+) is 1.3 for as-prepared Cit-AuNPs (Figure S11B, Supporting Information), and we fit this ratio with seven molecules of deprotonated acetoacetic acid per unit of configuration A (see the Supporting Information). However, we should mention that the disordered configuration may exist to some extent.

Notably, the interaction of the two hydrogen bonds of the free COOH groups is far stronger (total ∼28 kcal/mol; ∼7 kcal/mol per hydrogen bond of carboxylic acid dimers at room temperature)[92] than the single COO−Au interaction (∼2 kcal/mol).[93] In this case, the intermolecular interaction precedes the molecule−metal interaction. An interesting consequence of the citrate trimer is the formation of a citrate bilayer. We consider that the adsorbed citrate species in direct contact with the AuNP surface comprise the first layer and the dangling citrate species hydrogen-bonded with two adsorbed citrates make up the second (outer) layer.

Previously, only the free COO^- groups of adsorbed citrate were considered as the source of negatively charged surfaces of citrate-capped MNPs.[16] However, our study indicates that the negatively charged outer layer resulting from the central COO^- groups of the dangling citrate anion may be the origin of the well-known electrostatic repulsion of Cit-AuNPs. The orientation of the central COO^- group, i.e., pointing toward the metal surface or pointing outward, is not clear. The behavior of the central COO^- and OH groups in the outer layer may play an important role in NP stability and interparticle-type interactions between Cit-AuNPs in solution. A better understanding of the configuration of the dangling citrate layer may provide a foundation for more detailed studies about the effects of molecular conformation and adsorption on the electrical double layer at AuNP surfaces.

Sterically Stabilized AuNPs Due to the Citrate Layer. Cit-AuNPs are known to be electrostatically stabilized due to adsorption of citrate trianions ($citrate^{3-}$). Experimental evidence suggests that steric repulsion of citrate layers plays a role in stabilizing AuNPs.[12,94,95] The proposed structure of the citrate layer in our study also provides a basis for the possible role of steric stabilization in that negatively charged carboxylate groups of citrate anions adsorbed on AuNPs are shielded by hydrogen bonding between citrate anions after protonation. We attempted to measure the thickness of the citrate layer experimentally in solution to investigate the presence of short-range repulsive forces, i.e., steric repulsion rather than electrostatic repulsion, of the citrate layer.

We used (1,*n*)-alkanedithiols ($HS-(CH_2)_n-SH$, n = 3, 4, 5, 6, 9, 11) as molecular capping agents and probed AuNP aggregation. Since one thiol group of dithiols bind to a metallic surface of a single AuNP and the other thiol can bind to that of another AuNP, dithiols can act as molecular linkers to connect two different AuNPs.[96] When the hydrocarbon length of a dithiol is long enough for both sulfur atoms to adsorb on two different AuNPs, NPs are expected to be aggregated in solution beyond steric repulsion from the citrate layers of two different NPs (interparticle-type adsorption). When the hydrocarbon length of a dithiol is too short for both sulfur atoms to bind surfaces of different NPs simultaneously, AuNPs remain as single NPs in solution without aggregation (intraparticle-type adsorption). Although both sulfur atoms of alkanethiols can bind to the same surface (lying-down configuration), there is expected to be a population of dithiols with only one sulfur atom adsorbed on the surface (upright configuration) at a high concentration of the dithiol.[97] Interestingly, a dithiol length-dependent stability of AuNPs was observed. Figure 7 shows the stability of AuNPs in

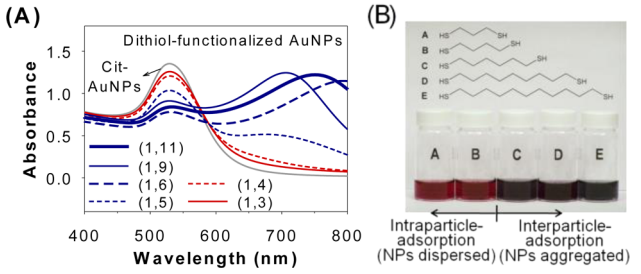

Figure 7. Molecular length-dependent stability of Cit-AuNPs upon addition of alkanedithiols with varied hydrocarbon length: (A) UV−vis absorbance spectra of Cit-AuNPs in solution after addition of (1,*n*)-alkanedithiols; (B) photograph of the solutions of AuNPs showing the change of AuNP stability due to dithiol length-dependent interparticle interactions. The solution of (1,5)-dithiol-AuNPs is omitted for clear visualization.

solution upon addition of dithiols with varied alkane chain lengths. When the length of alkanedithiols is short (for n = 3, 4), NPs are not aggregated and remain dispersed in solution. We observed the characteristic reddish color of stable AuNPs that exhibit a band of a localized surface plasmon resonance (LSPR) at 535 nm. When the length of alkanedithiols is longer (for n = 5, 6, 9, 11), however, NPs exhibit aggregation characterized by a strong red-shift of the surface plasmon (SP) band. Once the dithiols are long enough to span beyond the citrate layers and bind to different NPs, the AuNPs aggregate. The extent of the electrostatic repulsion between NPs does not change, because ionic strengths are constant due to the same concentrations of dithiol solutions (1 mM) added into the AuNP solution.[98] Under the high thiol concentration, the electrostatic repulsion may be negligible. Also, the IR data indicate the presence of citrate layers on AuNPs after the addition of dithiols regardless of the length.[69] This length-dependent adsorption of alkanedithiols on the

dx.doi.org/10.1021/ja4097384 | J. Am. Chem. Soc. 2014, 136, 1907−1921

surfaces of different AuNPs confirms that steric repulsion of the citrate layer plays a critical role in the stability of AuNPs.

On the basis of the interparticle interaction depending on the length of dithiols, the thickness of the citrate layer in solution could be estimated. Only the rigid layer of citrate anion renders NPs stabilized sterically under these experimental conditions (Figure 6A), and the effect of the disordered layer on steric stabilization is assumed to be negligible due to the flexibility of noninteracting terminal carboxyl groups and partially hydrogen-bonded dangling citrate anions (Figure 6B). There are two distinct steps of stability transition, one from (1,4)- to (1,5)-dithiol and the other from (1,5)- to (1,6)-dithiol (Figure 7). The calculated interparticle spacings are 12.6 Å for (1,4)-dithiol, 13.7 Å for (1,5)-dithiol, and 15.1 Å for (1,6)-dithiol, including the Au−S bond length (see the Supporting Information). We did not consider the tilt angle of ordered alkanethiol layers from the surface normal in determining the interparticle spacing. NPs exhibit the characteristic bluish color of aggregates, if any, within 10 min upon addition of dithiols. Thus, it is reasonable to assume that the interparticle-type adsorption of alkanedithiols is random in the short period of time. Disordered dithiol layers produce the maximum interparticle spacings.

A minimum thickness of the citrate layer falls between the lengths of (1,4)-dithiol and (1,5)-dithiols, which is in the range of 6.3−6.8 Å, including the Au−O_{COO} bond length. We attribute this minimum value to a van der Waals (vdW) barrier of the backbone of adsorbed species (6.6 Å, Figure S15, Supporting Information). The optimized thickness for vdW attraction is 6.7−6.8 Å. The presence of a sterically dominating single layer of citrate in the region of the AuNP surface indicates the disordered citrate layer exists (Figure 6B), likely in edge and vertex sites of AuNPs.

A second transition in nanoparticle aggregation from (1,5)- to (1,6)-dithiol is distinct as shown by the greater amplitude and red-shift of the LSPR peak related to aggregation, indicating the interparticle spacing through adsorption of (1,6)-dithiol exceeds the steric barrier of the entire citrate layer. The thickness of a hard-wall surface of the citrate layer is in the range of 6.9−7.6 Å. We attribute this value to a thickness of the ordered citrate configuration (Figure 6A) due to evidence of a cooperative interaction between citrate layers. The extent of the red-shift of the SP band is consistent with different aggregation kinetics depending on the dithols that are incorporated. The NPs aggregate immediately after addition of (1,6)-dithiol, whereas the NPs aggregate slowly for (1,9)- and (1,11)-dithiols. This suggests that the interparticle spacing close to 15.1 Å lies within the range of an interlayer interaction through dangling citrate anions that are in close proximity with each other, which can lead to the instantaneous NP aggregation observed in this study. Therefore, the thickness of the ordered citrate layer is ∼7.6 Å. The kinetics of NP aggregation upon addition of (1,7)- and (1,8)-alkanedithiols would offer a finer range of the layer thickness, but it is expected that the spacing would be less than that for (1,9)-alkanedithiol (9.5 Å), and this seems to be the upper limit. This conclusion is based on the observation that (1,9)-dithiol functionalized Cit-AuNPs exhibit a less red-shifted SP band and slower aggregation compared to (1,11)-dithiol functionalized Cit-AuNPs, indicating vdW repulsion between citrate layers plays a role in the case of (1,9)-dithiol. Thus, it can be concluded that the layer thickness is in the range of 8−10 Å. The relatively thin layer suggests dangling citrate anions are in close proximity to the metal surface. A layer thickness can be up to ∼14 Å if the terminal −COOH groups of adsorbed anions, which are hydrogen-bonded with dangling anions, are normal to the surface. The central carboxyl and hydroxyl groups of dangling anions may be oriented away from the metal surface for possible interlayer hydrogen bonding.

Grieser and co-workers demonstrated the existence of an uncharged surface species on Cit-AuNPs, and they also measured the barrier size for surface citrates to be 10 ± 2 Å in acidic pH and 7 ± 2 Å in basic pH, respectively.[12] This can be related to the formation of the citrate layer proposed in our study. In basic pH, dangling citrate anions are removed from adsorbed citrate, which can lead to a thickness of 7 Å, i.e., the vdW barrier of the citrate backbone. In acidic pH, the barrier size is 10 ± 2 Å, and the lower limit is in good agreement with our result. In our measurement, interlayer hydrogen bonding plays a role at a close interlayer distance, aided by the interparticle-type adsorption of alkanedithiols. This results in the narrow thickness. Mulvaney and Giersig[99] also estimated the thickness of the citrate layer on AuNPs as ∼5 Å with directly measuring the interparticle spacing of a closely packed NP 2-D array at a positive voltage. This value is comparable with the measured thickness of the citrate layer in our study. In their case, the applied potential may contract the citrate layer leading to a slightly smaller observed thickness.

From the abrupt transition of AuNP stability due to the dithiol length difference by one methylene unit, we can infer that the thickness of the citrate layer may be uniform over the entire surface of AuNPs. This helps support the possibility of the configurational similarity of the citrate trimer on the surfaces of the AuNPs as represented in Figure 6A. The intermolecular distance between two adsorbed citrate anions and subsequent height of the dangling citrate anions from the surface can be fairly uniform regardless of AuNP facets. Thus, we can consider the configuration of the citrate trimer as a building block on the AuNP surface, and this is discussed below.

Assembly of Dihydrogen Citrate Anions on a Au(111) Surface. Based on the spectroscopy results, we used structure-based modeling to consider a configuration for self-assembly of dihydrogen citrate anions ($H_2Citrate^-$) using a citrate trimer as a building block. Direct determination of the spacing between adsorbed citrate species and the corresponding organization of citrate trimers on AuNPs are beyond the capability of the analytical tools used in this study. However, we have considered the published STM results from Bai and co-workers.[85] The STM image of citrate on a gold (111) surface provides evidence of the orientation and intermolecular interaction between citrate anions which also can be applied to understand the citrate adsorption on the facets of AuNPs. Bai and co-workers interpreted the bright spots as each carboxylate group of the adsorbed citrates on the STM image,[85] but the resultant lateral size of the proposed citrate structure is about twice as large as the expected molecular dimension. Instead, we have interpreted the STM image of the citrate anions on Au(111) in a different way and assumed each bright spot is an isolated citrate species. Based on this assumption, a trimer unit can be identified as a building block for the organization of citrates, which consists of three bright spots aligned to the [211] direction on a Au(111) surface (Supporting Information, Figure S16).

More recent experimental evidence indicated that the interlayer spacing of citrate layers on AuNPs is 3.0−3.5 Å, obtained from atomic-resolution TEM images.[90] This very small value beyond the limit of vdW repulsion (4.2 Å)[100] between citrate molecules implies that there should be a specific configuration between citrate layers. We attributed the interlayer spacing to be a consequence of a specific orientation of citrate

dx.doi.org/10.1021/ja4097384 | J. Am. Chem. Soc. 2014, 136, 1907−1921

functional groups involving interlayer interaction. The plane of COOH dimers formed between adsorbed and dangling citrate anions is significantly tilted from the surface normal and oriented at an angle of ~25° from the surface (see the Supporting Information, Figure S17). This is consistent with the narrow thickness of the citrate bilayer measured in our study (8−10 Å). Also, the TEM observation of molecular layers may indicate that the citrate layer is well-organized on the AuNP surface.

By using conformation Ib as the adsorbed citrate (Figure 5B), specific directions of both terminal COOH groups are determined on Au(111), and two possible conformers were generated (Figure 8A). The terminal COOH groups at the C_3 position are oriented at ~25° from the surface and are hydrogen-bonded with dangling anions through formation of cyclic COOH dimers. The other terminal COOH groups at the C_1 position are parallel to the surface and are hydrogen-bonded with an adjacent adsorbed anion through formation of acyclic COOH dimers, evidenced by IR data (Figure 4B).

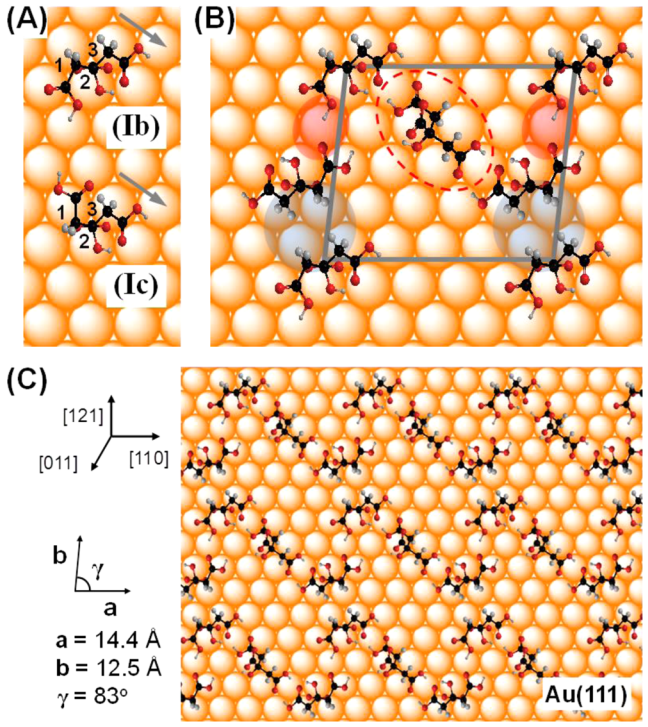

Figure 8. Model of the assembly of $H_2Citrate^-$ anions on a (111) surface of AuNPs. (A) Two possible conformers of adsorbed citrate. The COOH groups at C_1 are parallel to the surface while the COOH groups at C_3 (gray-arrowed) are oriented at the angle of ~25° from the surface. (B) Intermolecular interactions between citrate anions. Red circle: acyclic COOH hydrogen bonding between adsorbed anions, blue circle: van der Waals attraction of CH_2 moieties, red dotted line: a dangling anion, which is hydrogen-bonded with two adsorbed anions through formation of cyclic COOH dimers. Surface gold atoms are depicted as a space-filling model. The parallelogram represents a unit cell. (C) Proposed citrate self-assembly through the configuration of 1-D chains on Au(111) surface. Values are unit cell parameters.

We simulated adsorption of the citrate layer on the surface of AuNPs using the citrate trimers as building blocks (Figure 8B,C). We adapted the periodicity of the image pattern of citrate from the STM image published by Bai and co-workers (Figure S16, Supporting Information).[85] Adsorption of the citrates as the conformer Ib leads to the best fit with the published STM image of citrates adsorbed on Au(111) in terms of the orientation of the hydrogen-bonded COOH groups (Figure 8B), which can stabilize the molecular assembly. However, the length parameters should be increased by one gold atom distance (Figure 8C; see the Supporting Information, Figure S18 and S19). It seems that the hydroxyl group is hydrogen-bonded with both of the terminal COOH groups and stabililzes the syn conformation of conformer Ib. Both methylene moieties are placed on the same side. The anti conformation of conformer Ic may not be stable due to vdW repulsion between COOH at the C_1 position and $-CH_2-$ at the C_3 position.

Heinz and co-workers concluded that molecular adsorption is governed by molecular size and geometry rather than specific interfacial chemistry, investigated by molecular dynamics simulation for adsorption of single amino acids and surfactant molecules on Au(111).[101] In our modeling, we also considered the geometric coordination of the adsorbed citrate species with respect to the direction and spacing of the top lattice of the Au(111) surface, and we were not able to take into account other parameters including water solvent, additional anions/cations,[102] surface reconstruction,[103] and surface charges.[16] Interestingly, adsorption of the central COO^- groups at bridged sites[104] was exclusively observed in our modeling. Heinz and co-workers found that polarizable atoms including oxygen atoms of carboxylate groups are drawn into attractive epitaxial sites, i.e., bridged and 3-fold hollow sites, having deep potential wells due to the high surface energy of the metal.[101] This is consistent with citrate adsorption on Au(111) in our structure-based modeling. It is surprising that the formation of two hydrogen bonds (total ~14 kcal/mol) cannot precede two Au-carboxylate interactions (total ~4 kcal/mol) (Figure S20, Supporting Information). This suggests a stronger adsorption energy of entire citrate anions than ~2 kcal/mol, due to a significant contribution from other molecular fragments to the surface adsorption in addition to the direct chemical bonding (a calculated adsorption energy of a $citrate^{3-}$ anion: 8−10 kcal/mol).[101]

For modeling using a citrate trimer, we incorporated dangling citrate anions in the citrate layer. The configuration of the dangling citrate species ($H_2Citrate^-$) between two adsorbed species was obtained from one of the most stable and stretched conformations by ChemBio3D, having both terminal COOH groups parallel to each other. The central carboxylate groups of dangling citrate are uncoordinated. It is not clear whether the central carboxylate group points toward the metal surface or points outward. The direction of both hydrogen-bonded COOH groups with a dangling anion is parallel with each other in most trimers of the STM image, but a slight deviation from this orientation also was observed as a minor configuration (see the Supporting Information, Figure S21). The modeling also indicates that the presence of the dangling citrate species is plausible in the formation of a citrate trimer. A combination of three adsorbed citrate anions as a trimer unit is not commensurate on the surface (see the Supporting Information, Figure S22). The presence of a dangling citrate species is similar to the report of that for glutamic acids stabilized at ~4.6 Å above a silver surface without being in direct contact with the surface which is based on STM imaging.[105] Although citrate is not a chiral molecule, the overall assembly pattern generates chirality. Dangling citrate anions, aligned along the [101] direction rather than the [011] direction, were observed in the modeling (Figure 8C). It has been demonstrated that adsorption of one chirality induces the adsorption of homochirality,[106] and intermolecular hydrogen bonds[107] play an important role in chiral self-

dx.doi.org/10.1021/ja4097384 | J. Am. Chem. Soc. 2014, 136, 1907−1921

assemblies on metal surfaces. Overall, the model of citrate adsorption presents 1-D citrate chains consisting of adsorbed and dangling $H_2Citrate^-$ anions, which are all hydrogen-bonded along the [110] direction.

The gold atom spacing (a_o) is 2.88 Å.[101] The length parameters (a) and (b) in the unit cell are 14.4 Å ($5a_o$ = 14.4 Å) and 12.5 Å ($\sqrt{19}a_o$ = 12.5 Å), respectively, and the angle (γ) of the unit cell is 83°. The area of this unit cell is 179 Å^2. The O−H···O distance of the adjacent adsorbed citrate involving acyclic COOH hydrogen bonds is 2.7 Å, and this distance is optimized within a 0.1 Å deviation.[108] The distance between two adsorbed citrates connected with a dangling citrate anion is 13.6 Å. Interestingly, we found from the model that the CH_2 moieties are close with a spacing of 5.0 Å ($2a_o\cos30°$ = 5.0 Å) (Figure 8B). In order for the presented model to be correct, one must assume this proximity of CH_2 groups for vdW contact. Due to the citrate−Au surface interaction, the spacing of the CH_2 moieties of the adsorbed citrates is larger than that of the optimized vdW interaction (4.4−4.6 Å).[109] A similar value for CH_2 spacing was reported for glutamic acids on Ag(100) separated by 5.4 Å in a upstanding configuration.[110] Our model also is consistent with the measured thickness of the citrate layer (see the Supporting Information, Figure S23). The terminal COOH groups between adsorbed anions can bind to the surface by η^1-COO^- coordination (Figure S24, Supporting Information), and this process is reversible. The coordination transformation of the terminal COOH group likely depends on the specific NP facets or boundaries such as edge and vertex sites. In general, hydrogen bonds are not observed in STM imaging due to low electron density,[111] and this binding transformation cannot be distinguished by STM analysis.

There are indications of citrate chains on gold surfaces in the literature. AFM force measurements demonstrated the presence of a citrate network on a planar gold surface, possibly due to intermolecular hydrogen bonding.[112] Another AFM force measurement for citrate layers between a AuNP and a planar gold substrate suggested a neutral hydrogen-bonded network consisting of dihydrogen citrate molecules due to the low charge density and possible multilayer adsorption on the surface.[91] Formation of citric acid chains also was observed in aqueous solution.[113] Formations of carboxylic acid dimers[114] and clusters[115] in aqueous solution were demonstrated although these reports are controversial.[108] Due to preadsorbed citrate species on the surface during the synthesis of AuNPs, incorporation of citrate anions in solution into the formation of a citrate network within the electrical double layer on the AuNP surfaces is feasible.

We expect the driving forces for molecular assemblies of citrate to be both vdW interactions (−CH_2−···−CH_2− interaction: 0.8 kcal/mol, determined for alkanethiols on gold surfaces)[116] and hydrogen bonds of carboxylic acid groups (~14 kcal/mol per carboxylic acid dimer at room temperature).[92] An enthalpic gain can govern the adsorption of $H_2Citrate^-$ anions on the AuNP surface. Conformational entropy losses upon adsorption may be negligible[117] when the central COO^- and the hydroxyl groups form intramolecular hydrogen bonding and $H_2Citrate^-$ anions are intermolecular-hydrogen-bonded through terminal −COOH groups prior to adsorption. Due to the weak nature of the Au−carboxylate interaction, it is plausible to conclude that the citrate adsorption is driven by the intermolecular interactions, and the molecule-surface interaction is of secondary importance.[86] In order to promote the intermolecular interactions, it is necessary for citrate anions to diffuse on the Au surface since the carboxylate group does not readily adsorb on Au as it does on silver and copper.[84] Deprotonated carboxylate (COO^-) groups rather than −COOH bind on Au(111).[118] The adsorption of trimethylacetic acids (TMAA) on TiO_2(110) surface has been studied in detail at a molecular level. TMAA diffuses on the surface because of physisorption through COOH binding, and chemisorbed TMMA species resulting from O−H cleavage does not diffuse at room temperature and forms long-range ordering.[119] A similar mechanism can be applied for adsorption of citrate anions on the Au surface. Physisorbed citrate anions probably diffuse on the surface, and the central COO^- groups of citrate bind to the surface after favorable molecular interactions are achieved. It was reported that diffusion plays an important role in cysteine adsorbed on Au(111).[120] $H_2Citrate^-$ anions possessing the bidirectional −COOH groups likely diffuse to form the 1-D citrate chains on the surface, and then the bidirectional −CH_2− fragments of two adjacent adsorbed citrate anions promote the interchain interaction through vdW attraction for the 2-D structure of citrate layers.

Citrate Chains As Building Blocks on Other Facets of AuNPs. The Au(111) surface is the most populated facet in a large AuNP[37] due to having the lowest surface energy,[121] and there are other facets including Au(110) and Au(100) for the face-centered cubic structure in the truncated octahedron of large-sized AuNPs (>10 nm).[37,122,123] We adapted adsorption of the 1-D citrate chain to Au(110) and Au(100) surfaces to investigate the possibility of the citrate chain as a building block on those surfaces. Binding configuration of carboxylate oxygen atoms on Au(100) is adapted from the modeling result from Au(111), in which the oxygen atoms bind in bridge sites. Also, spacing of methylene moieties, which should not exceed the limit of vdW contact (4.2 Å),[100] was considered. On Au(110), a random orientation of coordinated COO^- moieties was reported,[124] and we used the binding of two oxygen atoms[39] in neighboring atomic rows along the [001] direction although the row spacing ($\sqrt{2}a_o$) is relatively large compared to the O···O distance (2.4 Å). Surprisingly, the citrate chain also fit to the surfaces of Au(110) and Au(100) with the same configuration of vdW and hydrogen bond interactions (Figure 9; see also Figure S25 in the Supporting Information for excluded assembly models). Dangling citrate anions form cyclic −COOH dimers with adsorbed anions. The distances between the two α-carbons of the COOH groups in the adjacent adsorbed citrates (~$2a_o$ = 5.8 Å) are shorter than the optimized value of cyclic COOH dimerization (6.8 Å)[108] for both surfaces, and each COOH molecular axis should be deviated from the parallel orientation, in order to form acyclic COOH dimers. The CH_2 spacings for vdW contact are ~5.8 Å (~$2a_o$ = 5.8 Å) on both surfaces. The intermolecular spacings along the dangling anions are 13.3 Å and 12.7 Å on (110) and (100) surfaces, respectively. Rodes and co-workers reported the ν(C═O) centered at ~1720 cm^{-1}, from

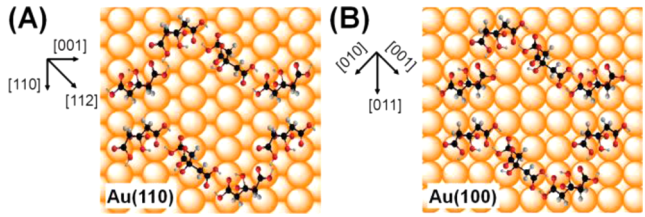

Figure 9. Proposed self-assemblies of citrate anions on (A) (110) and (B) on (100) surfaces of AuNPs.

dx.doi.org/10.1021/ja4097384 | J. Am. Chem. Soc. 2014, 136, 1907−1921

succinate anions ($^{-}OOCCH_2CH_2COO^{-}$) adsorbed on (111), (110), and (100) planar gold surfaces in acidic conditions.[39] This suggests the formation of COOH hydrogen bonding between adsorbed succinate anions is identical on those surfaces, which supports the hydrogen bonding through terminal COOH groups between adjacent citrate anions on (110) and (100) surfaces of AuNPs in this study. Obtaining STM images of citrate adsorption on the Au(110) and Au(100) surfaces would verify the self-assembly through the 1-D chain network. This is an example of a building block on one facet fitting to another. It has been reported that the self-assembled uracil on Au(111) exhibits identical packing on Au(100).[125] Based on the proposed adsorption model of citrate layers on (111), (110), and (100) surfaces of AuNPs, surface coverage including dangling citrate anions is $\sim 2.8 \times 10^{-10}$ mol/cm^2 (~45% coverage). This relatively low coverage of citrate anions on AuNPs is consistent with the speculation by Nelson and Rothberg, based on their investigation of DNA adsorption on Cit-AuNPs[126] (see the Supporting Information for further discussion).

Although the modeling result suggests the possible adsorption of 1-D citrate chains on Au(110) and Au(100) surfaces, the formation of the citrate layer on Au(110) may not be kinetically favorable. In general, molecules on the (110) metal surface diffuse exclusively along the [110] direction,[127] and thus the diffusion of citrate anions on Au(110) likely occurs in the [110] direction. This 1-D surface diffusion on Au(110) does not favor the formation of the 2-D citrate network relying on intermolecular interactions. On the Au(100) surface, however, the anisotropic diffusion does not take place, and the enthalpy factor of the intermolecular interaction may govern the citrate adsorption. Using our modeling result of the citrate adsorption on gold surfaces, it is also possible to take kinetics into consideration in the role of the citrate layer in stabilizing facets of citrate-based AuNPs.

Stabilization Role of the Citrate Layer on Surfaces of AuNPs via Intermolecular Interactions. Finally, we correlate the facet-dependent adsorption of citrate anions with the stabilizing effect of citrate layers on the surfaces of AuNPs. The modeling results of the size match between the citrate chain and gold surfaces indicate that citrate adsorption is optimized on Au(111). Adsorption of the hydrogen-bonded citrate chain also fits on Au(100), but adsorption preference among those surfaces is difficult to determine by our modeling. A difference in adsorption strength of the citrate layer between (111) and (100) surfaces, if any, may arise due to the spacing between adjacent adsorbed citrates due to vdW attraction which is more optimized on Au(111). A role of vdW attraction was demonstrated for polyvinylpyrrolidone (PVP) adsorption on Ag(111), which is a consequence of the high density of surface atoms on the (111) surface.[128] It is not clear whether the vdW contact differentiates the adsorption strength significantly for citrate anions. Although the configuration of the 2-D citrate adsorption is also commensurate on Au(110), the anisotropic molecular diffusion can deter the formation of the citrate network. Overall, the adsorption strength of the citrate layer is expected to decrease in the order Au(111) $\geq$ Au(100) > Au(110).

The order of the adsorption strength of the citrate layer on those gold surfaces is consistent with the ratio of exposing facet on AuNPs in that the (111) surface is the most populated facets on AuNPs followed by the (100) surface. Thermodynamic modeling[37] as well as TEM[122] and XRD[123] empirical evidence show that (111) and (100) surfaces are dominant for spherical Cit-AuNPs. The Au(110) surface is the least dominant surface showing the largest surface energy[121] among those low-index surfaces. It seems that the thermodynamically favored morphology (i.e, spherical shape or truncated octahedron structure) of Cit-AuNPs is supported by the stabilizing role of the citrate layer on the (111) and (100) surface. For those dominant surfaces, we assume that the weak Au−carboxylate interaction (2 kcal/mol, 0.087 eV) does not modify the surface energy difference ($\Delta\varphi_{(100)-(111)}$ > 0.1 eV),[129] for which surface energy is significantly altered through strong molecular adsorption (see the Supporting Information).[130] Occurrence of high energy surfaces such as (100) and (110) on AuNPs is possible only when those surfaces are stabilized by suitable stabilizers via adsorption-driven reversal of surface energies.[131] It has been demonstrated that rhombic dodecahedral AuNPs exclusively possessing the high-energy (110) facets can be synthesized when molecular surfactants stabilize those facets.[132] However, the low surface coverage on Cit-AuNPs, due to the formation of net-like structures of the citrate layer, allows citrate-based MNP seeds to offer surface energy reversal upon adsorption of other strongly binding additives including metal ions, halide ions, and amine-containing surfactants. The stabilization of the multisurfaces of Cit-AuNPs by the single fashion of the citrate adsorption can be related to the isotropic shape,[133] i.e., spherical, of the AuNP. The feasibility of the layer formation is extended to silver, platinum, palladium, and copper nanoparticles synthesized by the Turkevich method, and the role of citrate as a stabilizer is discussed in the Supporting Information (Figure S26).

Although it is possible that the entire citrate network is equally adsorbed on (111) and (100) surfaces of AuNPs, adsorbed citrate species show a preferential adsorption on Au(111). The structure-based modeling suggests adsorption of $H_2Citrate^{-}$ anions in bridge sites rather than atop sites. Adsorption geometry of citrate in bridge sites fits well on Au(111) (Figure 10). The

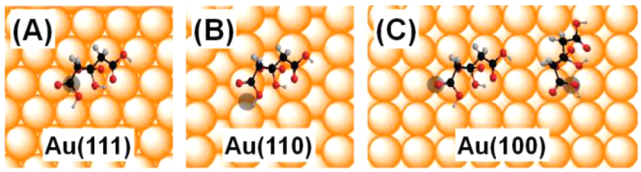

Figure 10. Binding of terminal carboxyl groups in bridge sites on (111), (110), and (100) surfaces of AuNPs. C_1 position is on the left side of the anion, and the COOH group at C_1 can be hydrogen-bonded with an adjacent adsorbed anion. η^1-COO^{-} binding at C_1 is possible only on Au(111). Two possible geometries are shown for Au(100). Blue circles represents proximal bridge sites for potential binding of the COOH group to the surface.

COOH orientation at the C_1 position may be stabilized at the bridge site on Au(111). This makes the hydrogen bonding with an adjacent anion more favorable due to the aligned orientation. Heinz and co-workers found that sp^3-hybridized molecular structures are preferentially adsorbed on Au(111) since the bond angle and length fit on the hexagonal lattice of the (111) surface.[102] Also, they suggest adsorption of polarizable atoms including C, O, and N atoms in bridge or hollow sites.[101] However, those terminal COOH groups on Au(110) and Au(100) locate at atop sites, likely oriented toward the surface normal due to a lack of the deep potential well. This orientation deviation may hinder the hydrogen bonding between adsorbed citrate anions on Au(110) and Au(100). If this is the case, the adsorption strength should decrease significantly in the order Au(111) $\gg$ Au(100) > Au(110). If a majority of citrate anions

form dimers prior to adsorption, this orientation effect will be diminished. More importantly, the η^1-COO^- binding of a terminal carboxyl group to a proximal bridge site is possible only on Au(111). Terminal COOH carbons at the C_1 position should locate near a bridge site rather than a top site in order to bind to the surface. Only the (111) surface is available for the η^1-COO^- binding. Terminal COOH carbons on Au(110) and Au(100) locate above the top sites and cannot bind in bridge sites. Note that the overall molecular geometry is optimized via vdW attraction. XPS analysis for purified Cit-AuNPs suggests that ~1/3 of COOH groups at one terminal position are uncoordinated, and this ratio is comparable with the ratio of facet areas for AuNPs (Au_{111}:Au_{100} = 78:22, based on an ideal truncated octahedron). This facet-dependent adsorption is valid for small molecules having a (1,2)-dicarboxylic acid fragment including amino acids, and likely affects adsorption and surface coverage of other incoming surfactants. The effects of the orientation of the terminal COOH at the C_1 position and its η^1-COO^- binding to the surface may be a key factor for anisotropic particle growth using citrate-based MNP seeds, under light irradiation, thermal treatment, electric potential, and chemical modification including pH changes as well as addition of halide ions, metal ions, and other surfactants.[134,135] The structural aspects of citrate adsorption on gold surfaces are applicable for other metal surfaces with similar lattice spacings such as silver. This structure-based analysis provides a detailed understanding of the preferential adsorption of (1,2)-dicarboxylic acid fragments on Ag(111) of silver nanoplates,[80] and the strong adsorption of succinate on a reconstructed Au(111) compared to malonate ($^-OOCCH_2COO^-$).[136]

CONCLUSION

We investigated the conformation of citrate layers on AuNP surfaces. ATR-IR, transmission FT-IR, XPS, as well as a structure-based simulation were employed, and those results are consistent with TEM and STM images of the citrate layer obtained from literature. Dihydrogen citrate anions ($H_2Citrate^-$) are adsorbed on the Au surface by η^2-COO^- coordination of the central carboxylate group. The adsorbed citrate interacts with an adjacent adsorbed species and a dangling citrate species through hydrogen bonds between the terminal carboxylic acid groups. The hydrogen-bonded $H_2Citrate^-$ anions produce 1-D citrate chains, which interact with each other through vdW attraction between proximal CH_2 moieties, leading to formation of a self-assembled layer of citrate molecules adsorbed on AuNP facets including (111), (110), and (100) surfaces. The estimated thickness of the citrate layer is 8−10 Å including the Au-COO^- bond length, which may depend on the facets of AuNPs. From the structure-based model of the citrate adsorption on Au(111), only syn conformers are expected to adsorb in bridge sites. With including the dangling citrates, the surface coverage becomes ~2.8×10^{-10} mol/cm^2. The monodentate citrate anions transform into tetradentate coordination upon binding of the hydroxyl and all carboxyl groups to the surface under basic conditions. The intermolecular interactions between citrate anions provide a molecular understanding of the observed steric repulsion between citrate layers for NP dispersion stability in solution and the facet-dependent stabilizing role of the entire citrate layer on surfaces of AuNPs. Considering hydrogen bonding, vdW attraction and surface diffusion as well as binding geometry of (1,2)-dicarboxylic acid fragments for citrate adsorption, we expected the formation of the citrate layer is favored on Au(111) but deterred on Au(110) and Au(100). The stability of citrate-stabilized silver, platinum, palladium, and copper NPs is consistent with the feasibility of the layer formation on those MNPs based on the structural model. The detailed study of the citrate layer on AuNPs is expected to provide new insights to help explain experimental observations from Cit-AuNP based studies as well as possibly for other citrate-stabilized MNPs, including seed-mediated particle growth. Also, the study of the coordination of carboxylate and hydroxyl groups of the adsorbed citrate on AuNP surfaces can provide insights for the binding structures of peptides,[102] amino acids,[137] and other small organic molecules[138] possessing carboxylic acid and/or hydroxyl functional groups on metal surfaces.

ASSOCIATED CONTENT

Supporting Information

Full experimental methods, supplementary discussion, additional IR, UV−vis, and XPS spectra, TEM images, and additional figures relating to the structure-based modeling. This material is available free of charge via the Internet at http://pubs.acs.org.

AUTHOR INFORMATION

Corresponding Author

shumaker-parry@chem.utah.edu

Notes

The authors declare no competing financial interest.

ACKNOWLEDGMENTS

We thank Dr. Brian van Devener from the Surface Analysis Laboratory at the University of Utah for assistance with XPS measurements. This work was supported by the National Science Foundation through an NSF Career Award (Grant No. CHE-0844764).

REFERENCES

(1) Turkevich, J.; Stevenson, P. C.; Hillier, J. *Discuss. Faraday Soc.* **1951**, 55−75.
(2) Frens, G. *Nature Phys. Sci.* **1973**, *241*, 20−22.
(3) Sardar, R.; Heap, T. B.; Shumaker-Parry, J. S. *J. Am. Chem. Soc.* **2007**, *129*, 5356−5357.
(4) Mirkin, C. A.; Letsinger, R. L.; Mucic, R. C.; Storhoff, J. J. *Nature* **1996**, *382*, 607−609.
(5) Xie, H.; Tkachenko, A. G.; Glomm, W. R.; Ryan, J. A.; Brennaman, M. K.; Papanikolas, J. M.; Franzen, S.; Feldheim, D. L. *Anal. Chem.* **2003**, *75*, 5797−5805.
(6) Brewer, S. H.; Glomm, W. R.; Johnson, M. C.; Knag, M. K.; Franzen, S. *Langmuir* **2005**, *21*, 9303−9307.
(7) Gearheart, L. A.; Ploehn, H. J.; Murphy, C. J. *J. Phys. Chem. B* **2001**, *105*, 12609−12615.
(8) Polte, J.; Ahner, T. T.; Delissen, F.; Sokolov, S.; Emmerling, F.; Thünemann, A. F.; Kraehnert, R. *J. Am. Chem. Soc.* **2010**, *132*, 1296−1301.
(9) Zhou, X.; Xu, W.; Liu, G.; Panda, D.; Chen, P. *J. Am. Chem. Soc.* **2010**, *132*, 138−146.
(10) Lin, S.-Y.; Tsai, Y.-T.; Chen, C.-C.; Lin, C.-M.; Chen, C.-H. *J. Phys. Chem. B* **2004**, *108*, 2134−2139.
(11) Mahmoudi, M.; Azadmanesh, K.; Shokrgozar, M. A.; Journeay, W. S.; Laurent, S. *Chem. Rev.* **2011**, *111*, 3407−3432.
(12) Biggs, S.; Mulvaney, P.; Zukoski, C. F.; Grieser, F. *J. Am. Chem. Soc.* **1994**, *116*, 9150−9157.
(13) Chow, M. K.; Zukoski, C. F. *J. Colloid Interface Sci.* **1994**, *165*, 97−109.
(14) Heard, S. M.; Grieser, F.; Barraclough, C. G.; Sanders, J. V. *J. Colloid Interface Sci.* **1983**, *93*, 545−555.
(15) Kimling, J.; Maier, M.; Okenve, B.; Kotaidis, V.; Ballot, H.; Plech, A. *J. Phys. Chem. B* **2006**, *110*, 15700−15707.

(16) Mpourmpakis, G.; Vlachos, D. G. *Phys. Rev. Lett.* **2009**, *102*, 155505.
(17) Ojea-Jiménez, I.; Romero, F. M.; Bastús, N. G.; Puntes, V. *J. Phys. Chem. C* **2010**, *114*, 1800−1804.
(18) Uppal, M. A.; Kafizas, A.; Ewing, M. B.; Parkin, I. P. *New J. Chem.* **2010**, *34*, 2906−2914.
(19) Ji, X.; Song, X.; Li, J.; Bai, Y.; Yang, W.; Peng, X. *J. Am. Chem. Soc.* **2007**, *129*, 13939−13948.
(20) Zhao, L.; Jiang, D.; Cai, Y.; Ji, X.; Xie, R.; Yang, W. *Nanoscale* **2012**, *4*, 5071−5076.
(21) Glusker, J. P. *Acc. Chem. Res.* **1980**, *13*, 345−352.
(22) Xia, X.; Xie, S.; Liu, M.; Peng, H.-C.; Lu, N.; Wang, J.; Kim, M. J.; Xia, Y. *Proc. Natl. Acad. Sci. U.S.A.* **2013**, *110*, 6669−6673.
(23) Lu, F.; Zhang, Y.; Zhang, L.; Zhang, Y.; Wang, J.; Adzic, R. R.; Stach, E. A.; Gang, O. *J. Am. Chem. Soc.* **2011**, *133*, 18074−18077.
(24) Ye, X.; Gao, Y.; Chen, J.; Reifsnyder, D. C.; Zheng, C.; Murray, C. B. *Nano Lett.* **2013**, *13*, 2163−2171.
(25) Willey, T. M.; Vance, A. L.; Bostedt, C.; van Buuren, T.; Meulenberg, R. W.; Terminello, L. J.; Fadley, C. S. *Langmuir* **2004**, *20*, 4939−4944.
(26) Max, J.-J.; Chapados, C. *J. Phys. Chem. A* **2004**, *108*, 3324−3337.
(27) Nara, M.; Torii, H.; Tasumi, M. *J. Phys. Chem.* **1996**, *100*, 19812−19817.
(28) Munro, C. H.; Smith, W. E.; Garner, M.; Clarkson, J.; White, P. C. *Langmuir* **1995**, *11*, 3712−3720.
(29) SERS data on silver nanoparticles: Siiman, O.; Bumm, L. A.; Callaghan, R.; Blatchford, C. G.; Kerker, M. *J. Phys. Chem.* **1983**, *87*, 1014−1023.
(30) Ataka, K.-I.; Osawa, M. *Langmuir* **1998**, *14*, 951−959.
(31) Norén, K.; Loring, J. S.; Persson, P. *J. Colloid Interface Sci.* **2008**, *319*, 416−428.
(32) Barth, A.; Zscherp, C. *Q. Rev. Biophys.* **2002**, *35*, 369−430.
(33) Ohe, C.; Ando, H.; Sato, N.; Urai, Y.; Yamamoto, M.; Itoh, K. *J. Phys. Chem. B* **1999**, *103*, 435−444.
(34) Du, X.; Liang, Y. *J. Phys. Chem. B* **2004**, *108*, 5666−5670.
(35) Cabaniss, S. E.; Leenheer, J. A.; McVey, I. F. *Spectrochim. Acta, Part A* **1998**, *54*, 449−458.
(36) Gerken, J. B.; Badger, C.; Bisbee, C.; Gardner, S.; Qi, Y.; Vilá, V. D.; Roberts, J. D. *J. Phys. Org. Chem.* **2008**, *21*, 193−197.
(37) Barnard, A. S.; Young, N. P.; Kirkland, A. I.; van Huis, M. A.; Xu, H. *ACS Nano* **2009**, *3*, 1431−1436.
(38) Rodes, A.; Pastor, E.; Iwasita, T. *J. Electroanal. Chem.* **1994**, *376*, 109−118.
(39) Delgado, J. M.; Berná, A.; Orts, J. M.; Rodes, A.; Feliu, J. M. *J. Phys. Chem. C* **2007**, *111*, 9943−9952.
(40) Matzapetakis, M.; Raptopoulou, C. P.; Tsohos, A.; Papaefthymiou, V.; Moon, N.; Salifoglou, A. *J. Am. Chem. Soc.* **1998**, *120*, 13266−13267.
(41) Dubois, L. H.; Zegarski, B. R.; Nuzzo, R. G. *Langmuir* **1986**, *2*, 412−417.
(42) Berná, A.; Delgado, J. M.; Orts, J. M.; Rodes, A.; Feliu, J. M. *Electrochim. Acta* **2008**, *53*, 2309−2321.
(43) Floate, S.; Hosseini, M.; Arshadi, M. R.; Ritson, D.; Young, K. L.; Nichols, R. J. *J. Electroanal. Chem.* **2003**, *542*, 67−74.
(44) Nichols, R. J.; Burgess, I.; Young, K. L.; Zamlynny, V.; Lipkowski, J. *J. Electroanal. Chem.* **2004**, *563*, 33−39.
(45) Delgado, J. M.; Blanco, R.; Orts, J. M.; Pérez, J. M.; Rodes, A. *Electrochim. Acta* **2010**, *55*, 2055−2064.
(46) Bieri, M.; Bürgi, T. *Langmuir* **2005**, *21*, 1354−1363.
(47) Huang, X.; Jiang, S.; Liu, M. *J. Phys. Chem. B* **2005**, *109*, 114−119.
(48) Peng, C. S.; Jones, K. C.; Tokmakoff, A. *J. Am. Chem. Soc.* **2011**, *133*, 15650−15660.
(49) Deng, Y.-F.; Zhou, Z.-H. *J. Coord. Chem.* **2009**, *62*, 1484−1491.
(50) Dietrich, G.; Krückeberg, S.; Lützenkirchen, K.; Schweikhard, L.; Walther, C. *J. Chem. Phys.* **2000**, *112*, 752−760.
(51) Gong, J.; Flaherty, D. W.; Ojifinni, R. A.; White, J. M.; Mullins, C. B. *J. Phys. Chem. C* **2008**, *112*, 5501−5509.
(52) Liu, X.; Xu, B.; Haubrich, J.; Madix, R. J.; Friend, C. M. *J. Am. Chem. Soc.* **2009**, *131*, 5757−5759.
(53) Diewok, J.; Ayora-Cañada, M. J.; Lendl, B. *Anal. Chem.* **2002**, *74*, 4944−4954.
(54) Lindegren, M.; Loring, J. S.; Persson, P. *Langmuir* **2009**, *25*, 10639−10647.
(55) Young, A. G.; Green, D. P.; McQuillan, A. J. *Langmuir* **2006**, *22*, 11106−11112.
(56) Camplin, J. P.; McCash, E. M. *Surf. Sci.* **1996**, *360*, 229−241.
(57) Jones, G. S.; Marrikakis, M.; Barteau, M. A.; Vohs, J. M. *J. Am. Chem. Soc.* **1998**, *120*, 3196−3204.
(58) Wu, G.; Stacchiola, D.; Kaltchev, M.; Tysoe, W. T. *Surf. Sci.* **2000**, *463*, 81−92.
(59) May, C. J.; Canavan, H. E.; Castner, D. G. *Anal. Chem.* **2004**, *76*, 1114−1122.
(60) Tielens, F.; Humbolt, V.; Pradier, C.-M.; Calatayud, M.; Illas, F. *Langmuir* **2009**, *25*, 9980−9985.
(61) Sastry, M.; Ganguly, P. *J. Phys. Chem. A* **1998**, *102*, 697−702.
(62) Dmitriev, A.; Spillmann, H.; Stepanow, S.; Strunskus, T.; Wöll, C.; Seitsonen, A. P.; Lingenfelder, M.; Lin, N.; Barth, J. V.; Kern, K. *ChemPhysChem* **2006**, *7*, 2197−2204.
(63) The O 1s binding energy is not as distinct as in the literature due to the presence of water and hydroxide ions in this study: Lin, N.; Payer, D.; Dmitriev, A.; Strunskus, T.; Wöll, C.; Barth, J. V.; Kern, K. *Angew. Chem., Int. Ed.* **2005**, *44*, 1488−1491.
(64) Petroski, J.; El-Sayed, M. A. *J. Phys. Chem. A* **2003**, *107*, 8371−8375.
(65) Linic, S.; Barteau, M. A. *J. Am. Chem. Soc.* **2002**, *124*, 310−317.
(66) Baran, E. J. *Spectrochim. Acta, Part A* **2007**, *66*, 114−117.
(67) Jakubowicz, A.; Jia, H.; Wallace, R. M.; Gnade, B. E. *Langmuir* **2005**, *21*, 950−955.
(68) Wang, S.; Yao, H.; Sato, S.; Kimura, K. *J. Am. Chem. Soc.* **2004**, *126*, 7438−7439.
(69) Park, J.-W.; Shumaker-Parry, J. S. To be submitted.
(70) Kawaguchi, S.; Kitano, T.; Ito, K. *Macromolecules* **1991**, *24*, 6030−6036.
(71) Lee, H. M.; Kumar, A.; Kołaski, M.; Kim, D. Y.; Lee, E. C.; Min, S. K.; Park, M.; Choi, Y. C.; Kim, K. S. *Phys. Chem. Chem. Phys.* **2010**, *12*, 6278−6287.
(72) Cézard, C.; Rice, C. A.; Suhm, M. A. *J. Phys. Chem. A* **2006**, *110*, 9839−9848.
(73) Mizukami, M.; Moteki, M.; Kurihara, K. *J. Am. Chem. Soc.* **2002**, *124*, 12889−12897.
(74) Imae, T.; Torii, H. *J. Phys. Chem. B* **2000**, *104*, 9218−9224.
(75) Häggman, L.; Lindblad, C.; Oskarsson, H.; Ullström, A.-S.; Persson, I. *J. Am. Chem. Soc.* **2003**, *125*, 3631−3641.
(76) Martin, R. B. *J. Phys. Chem.* **1961**, *65*, 2053−2055.
(77) Li, Z.; Han, B.; Wan, L. J.; Wandlowski, Th. *Langmuir* **2005**, *21*, 6915−6928.
(78) Williams, J.; Haq, S.; Raval, R. *Surf. Sci.* **1996**, *368*, 303−309.
(79) Olson, A. L.; Cai, S.; Herdendorf, T. J.; Miziorko, H. M.; Sem, D. S. *J. Am. Chem. Soc.* **2010**, *132*, 2102−2103.
(80) Zhang, Q.; Li, N.; Goebl, J.; Lu, Z.; Yin, Y. *J. Am. Chem. Soc.* **2011**, *133*, 18931−18939.
(81) Pearce, K. N.; Creamer, L. K. *Aust. J. Chem.* **1975**, *28*, 2409−2415.
(82) Glusker, J. P.; van der Helm, D.; Love, W. E.; Dornberg, M. L.; Patterson, A. L. *J. Am. Chem. Soc.* **1960**, *82*, 2964−2965.
(83) Kunze, J.; Burgess, I.; Nichols, R.; Buess-Herman, C.; Lipkowski, J. *J. Electroanal. Chem.* **2007**, *599*, 147−159.
(84) Paik, W.-k.; Han, S.; Shin, W.; Kim, Y. *Langmuir* **2003**, *19*, 4211−4216.
(85) Lin, Y.; Pan, G.-B.; Su, G.-J.; Fang, X.-H.; Wan, L.-J.; Bai, C.-L. *Langmuir* **2003**, *19*, 10000−10003.
(86) Teobaldi, G.; Zerbetto, F. *J. Phys. Chem. C* **2007**, *111*, 13879−13885.
(87) Lahann, J.; Mitragotri, S.; Tran, T.-N.; Kaido, H.; Sundaram, J.; Choi, I. S.; Hoffer, S.; Somorjai, G. A.; Langer, R. *Science* **2003**, *299*, 371−374.
(88) Silva, A. M. N.; Kong, X.; Parkin, M. C.; Cammack, R.; Hider, R. C. *Dalton Trans.* **2009**, 8616−8625.

(89) Kelley, A. T.; Ngunjiri, J. N.; Serem, W. K.; Lawrence, S. O.; Yu, J.-J.; Crowe, W. E.; Garno, J. C. *Langmuir* **2010**, *26*, 3040−3049.
(90) Lee, Z.; Jeon, K.-J.; Dato, A.; Erni, R.; Richardson, T. J.; Frenklach, M.; Radmilovic, V. *Nano Lett.* **2009**, *9*, 3365−3369.
(91) Wall, J. F.; Grieser, F.; Zukoski, C. F. *J. Chem. Soc., Faraday Trans.* **1997**, *93*, 4017−4020.
(92) Gao, Q.; Hemminger, J. C. *Surf. Sci.* **1991**, *248*, 45−56.
(93) Chen, F.; Li, X.; Hihath, J.; Huang, Z.; Tao, N. *J. Am. Chem. Soc.* **2006**, *128*, 15874−15881.
(94) Rodrígez-González, B.; Mulvaney, P.; Liz-Marzán, L. M. *Z. Phys. Chem.* **2007**, *221*, 415−426.
(95) Wagener, P.; Schwenke, A.; Barcikowski, S. *Langmuir* **2012**, *28*, 6132−6140.
(96) Brust, M.; Bethell, D.; Schiffrin, D. J.; Kiely, C. J. *Adv. Mater.* **1995**, *7*, 795−797.
(97) Wallner, A.; Jafri, S. H. M.; Blom, T.; Gogoll, A.; Leifer, K.; Baumgartner, J.; Ottosson, H. *Langmuir* **2011**, *27*, 9057−9067.
(98) Jiang, L.; Wang, W.; Fuchs, H.; Chi, L. *Small* **2009**, *5*, 2819−2822.
(99) Giersig, M.; Mulvaney, P. *Langmuir* **1993**, *9*, 3408−3413.
(100) Li, J.-L.; Car, R.; Tang, C.; Wingreen, N. S. *Proc. Natl. Acad. Sci. U.S.A.* **2007**, *104*, 2626−2630.
(101) Feng, J.; Pandey, R. B.; Berry, R. J.; Farmer, B. L.; Naik, R. R.; Heinz, H. *Soft Matter* **2011**, *7*, 2113−2120.
(102) Heinz, H.; Farmer, B. L.; Pandey, R. B.; Slocik, J. M.; Patnaik, S. S.; Pachter, R.; Naik, R. R. *J. Am. Chem. Soc.* **2009**, *131*, 9704−9714.
(103) Jewell, A. D.; Sykes, E. C. H.; Kyriakou, G. *ACS Nano* **2012**, *6*, 3545−3552.
(104) Noda, H.; Wan, L.-J.; Osawa, M. *Phys. Chem. Chem. Phys.* **2001**, *3*, 3336−3342.
(105) Smerieri, M.; Vattuone, L.; Costa, D.; Tielens, F.; Savio, L. *Langmuir* **2010**, *26*, 7208−7215.
(106) Parschau, M.; Romer, S.; Ernst, K.-H. *J. Am. Chem. Soc.* **2004**, *126*, 15398−15399.
(107) Naitabdi, A.; Humblot, V. *Appl. Phys. Lett.* **2010**, *97*, 223112.
(108) Chocholoušová, J.; Vacek, J.; Hobza, P. *J. Phys. Chem. A* **2003**, *107*, 3086−3092.
(109) Ulman, A. *Chem. Rev.* **1996**, *96*, 1533−1554.
(110) Smerieri, M.; Vattuone, L.; Kravchuk, T.; Costa, D.; Savio, L. *Langmuir* **2011**, *27*, 2393−2404.
(111) Iwai, H.; Egawa, C. *Langmuir* **2010**, *26*, 2294−2300.
(112) Larson, I.; Chan, D. Y. C.; Drummond, C. J.; Grieser, F. *Langmuir* **1997**, *13*, 2429−2431.
(113) Groen, H.; Roberts, K. J. *J. Phys. Chem. B* **2001**, *105*, 10723−10730.
(114) Chen, J.; Brooks, C. L., III; Scheraga, H. A. *J. Phys. Chem. B* **2008**, *112*, 242−249.
(115) Nishi, N.; Nakabayashi, T.; Kosugi, K. *J. Phys. Chem. A* **1999**, *103*, 10851−10858.
(116) Nuzzo, R. G.; Bubois, L. H.; Allara, D. L. *J. Am. Chem. Soc.* **1990**, *112*, 558−569.
(117) Gutzler, R.; Sirtl, T.; Dienstmaier, J. F.; Mahata, K.; Heckl, W. H.; Schmittel, M.; Lackinger, M. *J. Am. Chem. Soc.* **2010**, *132*, 5084−5090.
(118) Feyer, V.; Plekan, O.; Tsud, N.; Cháb, V.; Matolín, V.; Prince, K. C. *Langmuir* **2010**, *26*, 8606−8613.
(119) Lyubinetsky, I.; Deskins, N. A.; Du, Y.; Vestergaard, E. K.; Kim, D. J.; Dupuis, M. *Phys. Chem. Chem. Phys.* **2010**, *12*, 5986−5992.
(120) Mateo-Martí, E.; Rogrero, C.; Gonzalez, C.; Sobrado, J. M.; de Andrés, P. L.; Martin-Gago, J. A. *Langmuir* **2010**, *26*, 4113−4118.
(121) Singh-Miller, N. E.; Marzari, N. *Phys. Rev. B* **2009**, *80*, 235407.
(122) Wang, Z. L.; Mohamed, M. B.; El-Sayed, M. A. *Surf. Sci.* **1999**, *440*, L809−L814.
(123) Long, N. N.; Vu, L. V.; Kiem, C. D.; Doanh, S. C.; Nguyet, C. T.; Hang, P. T.; Thien, N. D.; Quynh, L. M. *J. Phys. Conf. Ser.* **2009**, *187*, 012026.
(124) Feyer, V.; Plekan, O.; Ptasińska, S.; Iakhnenko, M.; Tsud, N.; Prince, K. C. *J. Phys. Chem. C* **2012**, *116*, 22960−22966.
(125) Dretschkow, Th.; Dakkouri, A. S.; Wandlowski, Th. *Langmuir* **1997**, *13*, 2843−2856.
(126) Nelson, E. M.; Rothberg, L. J. *Langmuir* **2011**, *27*, 1770−1777.
(127) Weckesser, J.; Barth, J. V.; Kern, K. *J. Chem. Phys.* **1999**, *110*, 5351−5354.
(128) Saidi, W. A.; Feng, H.; Fichthorn, K. A. *J. Phys. Chem. C* **2013**, *117*, 1163−1171.
(129) Zhang, W.; Liu, Y.; Cao, R.; Li, Z.; Zhang, Y.; Tang, Y.; Fan, K. *J. Am. Chem. Soc.* **2008**, *130*, 15581−15588.
(130) McKenna, K. P. *Phys. Chem. Chem. Phys.* **2009**, *11*, 4145−4151.
(131) Cortes-Huerto, R.; Goniakowski, J.; Noguera, C. *J. Chem. Phys.* **2013**, *138*, 244706.
(132) Jeong, G. H.; Kim, M.; Lee, Y. W.; Choi, W.; Oh, W. T.; Park, Q-H.; Han, S. W. *J. Am. Chem. Soc.* **2009**, *131*, 1672−1673.
(133) Coppage, R.; Slocik, J. M.; Briggs, B. D.; Frenkel, A. I.; Heinz, H.; Naik, R. R.; Knecht, M. R. *J. Am. Chem. Soc.* **2011**, *133*, 12346−12349.
(134) Sau, T. K.; Rogach, A. L. *Adv. Mater.* **2010**, *22*, 1781-1804 and references therein.
(135) Grzelczak, M.; Pérez-Juste, J.; Mulvaney, P.; Liz-Marzán, L. M. *Chem. Soc. Rev.* **2008**, *37*, 1783-1791 and references therein.
(136) Skołuda, P. *J. Electroanal. Chem.* **2000**, *488*, 154−157.
(137) Hoefling, M.; Iori, F.; Corni, S.; Gottschalk, K.-E. *ChemPhysChem* **2010**, *11*, 1763−1767.
(138) Langner, A.; Tait, S. L.; Lin, N.; Chandrasekar, R.; Ruben, M.; Kern, K. *Angew. Chem., Int. Ed.* **2008**, *47*, 8835−8838.